Crystal structure and subsequent ligand design of a nonriboside partial agonist bound to the adenosine A2A receptor

Amelia, T.; Veldhoven, J.P.D. van; Falsini, M.; Liu, R.; Heitman, L.H.; Westen, G.J.P. van; ... ; IJzerman, A.P.

Journal of Medicinal Chemistry

pubs.acs.org/jmc

Article

Crystal Structure and Subsequent Ligand Design of a Nonriboside Partial Agonist Bound to the Adenosine A_{2A} Receptor

Tasia Amelia, Jacobus P. D. van Veldhoven, Matteo Falsini, Rongfang Liu, Laura H. Heitman, Gerard J. P. van Westen, Elena Segala, Grégory Verdon, Robert K. Y. Cheng, Robert M. Cooke, Daan van der Es, and Adriaan P. IJzerman*

Cite This: *J. Med. Chem.* 2021, 64, 3827−3842

Read Online

ACCESS | Metrics & More | Article Recommendations | Supporting Information

ABSTRACT: In this study, we determined the crystal structure of an engineered human adenosine A_{2A} receptor bound to a partial agonist and compared it to structures cocrystallized with either a full agonist or an antagonist/inverse agonist. The interaction between the partial agonist, belonging to a class of dicyanopyridines, and amino acids in the ligand binding pocket inspired us to develop a small library of derivatives and assess their affinity in radioligand binding studies and potency and intrinsic activity in a functional, label-free, intact cell assay. It appeared that some of the derivatives retained the partial agonist profile, whereas other ligands turned into inverse agonists. We rationalized this remarkable behavior with additional computational docking studies.

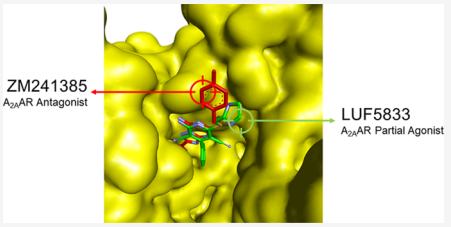

INTRODUCTION

Human adenosine receptors, of which there are four subtypes (hA_1AR, $hA_{2A}AR$, $hA_{2B}AR$, and hA_3AR), belong to the large superfamily of G protein-coupled receptors (GPCRs).[1] The $hA_{2A}AR$ was one of the first GPCRs crystallized;[2,3] multiple structures are available now, both with antagonists/inverse agonists or (full) agonists bound.[4] Typically and unlike prototypic antagonists such as ZM241385, agonists such as adenosine itself bear a ribose moiety, which is deemed critical for agonist activity (Figure 1).[5] The latter dogma was challenged by a series of dicyanopyridines without a ribose group, discovered, and further developed in the Bayer laboratories as partial agonists predominantly for the hA_1AR.[6,7] A recent phase 2b clinical trial with one of these compounds, neladenoson, failed to meet the primary endpoint in patients with heart failure, however.[8] Depending on the substitution pattern of these pyridine derivatives, affinity for A_{2A} and A_{2B} receptors can be achieved as well. Colotta and coworkers synthesized a number of derivatives with high affinity for $hA_{2B}AR$,[9] while BAY 60-6583 was reported to be a partial agonist for $A_{2B}AR$.[10] We ourselves synthesized **8** (LUF5833) and LUF5834 (Figure 1) with appreciable affinity for the adenosine A_{2A} receptor and partial agonistic activity on this receptor subtype.[11,12]

In this study, we present the crystal structure of **8** bound to an engineered construct of the adenosine A_{2A} receptor and compare this structure with those of antagonist- and agonist-bound receptors. We then synthesized a series of derivatives of **8** (Figure 1) inspired by the compound's interaction with specific amino acids in the binding pocket of the receptor. These novel compounds were evaluated in radioligand binding studies to assess their affinity for the (four) adenosine receptor subtypes. We also tested these compounds in a label-free impedance-based assay to determine their intrinsic activity on the A_{2A} receptor, revealing a huge variation in efficacy, in between agonism and inverse agonism. Further docking studies shed light on the atomic/structural features responsible for this behavior.

RESULTS

Structure of the Compound 8−Receptor Complex. To obtain crystals of the compound **8**−receptor complex, we used an existing thermostabilized receptor construct combined with a bRIL fusion protein, coined A_{2A}-StaR2-bRIL,[13] and a previously described approach in which crystals of A_{2A}-StaR2-bRIL were formed with theophylline.[14] After soaking the crystals with **8**, they were exposed to synchrotron X-ray radiation and diffraction data collected to 3.1 Å resolution (Figure 2A and Figure S1A). Following initial rounds of refinement using the receptor only, both residual $2F_o - F_c$ and $F_o - F_c$ electron density maps (Figure S1B) revealed clearly the entire pose of **8** and most surrounding side chains lining the binding site.

Compound **8** adopts an extended pose in the orthosteric binding site of $hA_{2A}AR$, engaging many of the residues

Received: November 11, 2020
Published: March 25, 2021

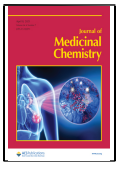

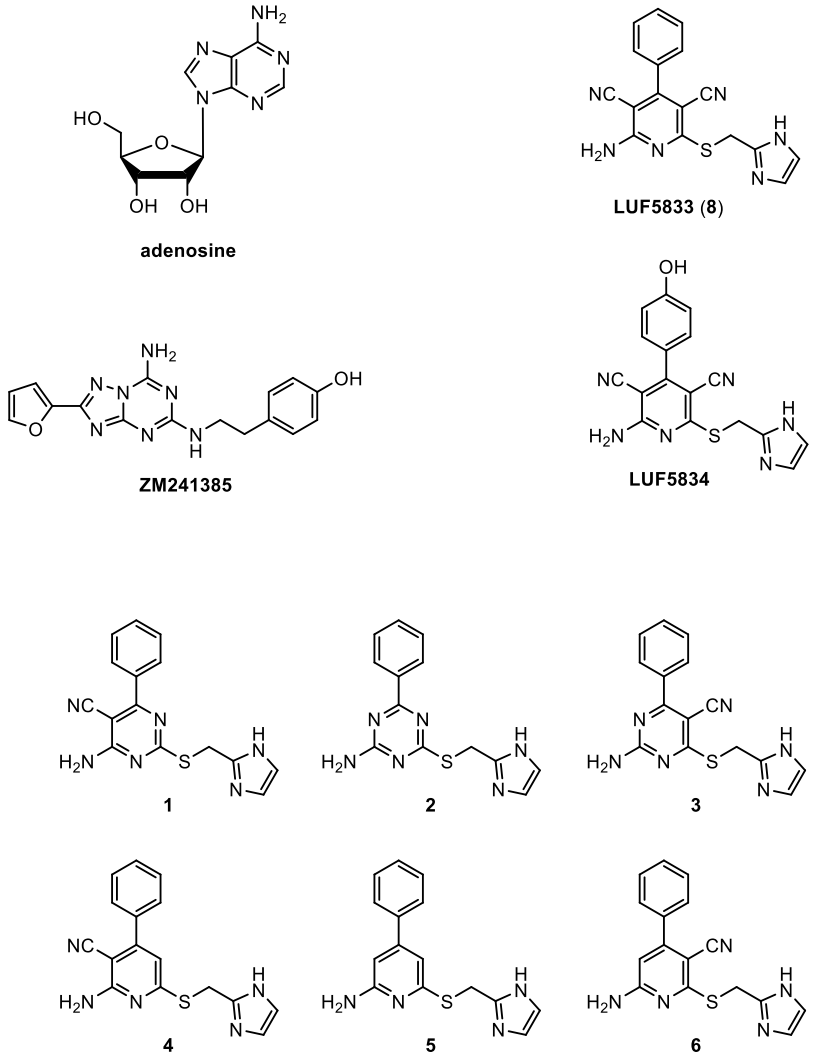

Figure 1. Chemical structures of adenosine, the nonriboside partial agonists **8** (LUF5833) and LUF5834, inverse agonist/antagonist ZM241385, and the derivatives of **8** synthesized in this study (**1**–**6**).

previously described as interacting with agonists and antagonists[13] (Figure 2B). The imidazole substituent lies nearest the extracellular face in a pocket lined by the side chains of Leu267$^{7.32}$, Met270$^{7.35}$, Tyr271$^{7.36}$, and Ile274$^{7.39}$ (superscript numbering according to Ballesteros and Weinstein[15]). The pyridine core is positioned similarly to the adenine moiety in NECA, lying between Ile274$^{7.39}$ and Phe168$^{5.29}$, and the phenyl group lies deepest in the receptor, similar to the ribose of adenosine, contacting Trp246 and forming a $\pi-\pi$ interaction with Phe168$^{5.29}$. One cyano substituent forms a hydrogen bond with Asn253$^{6.55}$ and the exocyclic amine interacts with Asn253$^{6.55}$ and Glu169^{EL2}.

Among the 19 amino acids close (<4 Å) to **8** (Figure 2C), Ser277$^{7.42}$ (Ala in A_{2A}-StaR2-bRIL; see Discussion and Conclusions) and His278$^{7.43}$ have been found crucial for full agonist binding.[16,17] For a further analysis of the latter, we compared this structure with two reference A_{2A} receptor structures, one antagonist/inverse agonist (ZM241385)-bound (PDB ID: 5IU4)[13] and the other agonist (NECA)-bound (PDB ID: 2YDV)[18] (Figures S2 and S3). The overall compound **8** and ZM241385 receptor structures were very similar (protein–protein RMSD, 0.65 Å), not unexpectedly since the same receptor construct was used in both. However, the amino acids making up the binding pocket of ZM241385 do not include "agonistic" Ser277$^{7.42}$ and His278$^{7.43}$, validating the antagonistic nature of ZM241385 (Figures S2A and S3A). Contrarily, the binding pocket around NECA's ribose moiety does include these two amino acids next to, e.g., Thr88$^{3.36}$, another amino acid known to be involved in full agonist activation[16,19] (Figures 2B and 3B). Although far from being conclusive on the basis of 3D architecture alone, this comparison between the three receptor structures suggests that the binding pocket of **8** shares characteristics of both agonist- and antagonist-occupied receptors. Hence, we decided to synthesize six derivatives of **8** to shed further light on the compound's agonistic/antagonistic behavior.

Synthesis of Compound 8 Derivatives. In these derivatives, the cyano groups and the number of nitrogen atoms in the core were varied (compounds **1**–**6**, Figure 1). Due to the targeted change in the core scaffold, a different synthetic pathway was used for every analogue of **8**. The synthesis routes toward the pyrimidine and triazine derivatives are shown in Scheme 1.

Compound **1** was synthesized starting with a multicomponent reaction between benzaldehyde (**9**), malononitrile, and thiourea, forming intermediate **10**.[20] Then, 2-bromome-

https://doi.org/10.1021/acs.jmedchem.0c01856
J. Med. Chem. 2021, 64, 3827–3842

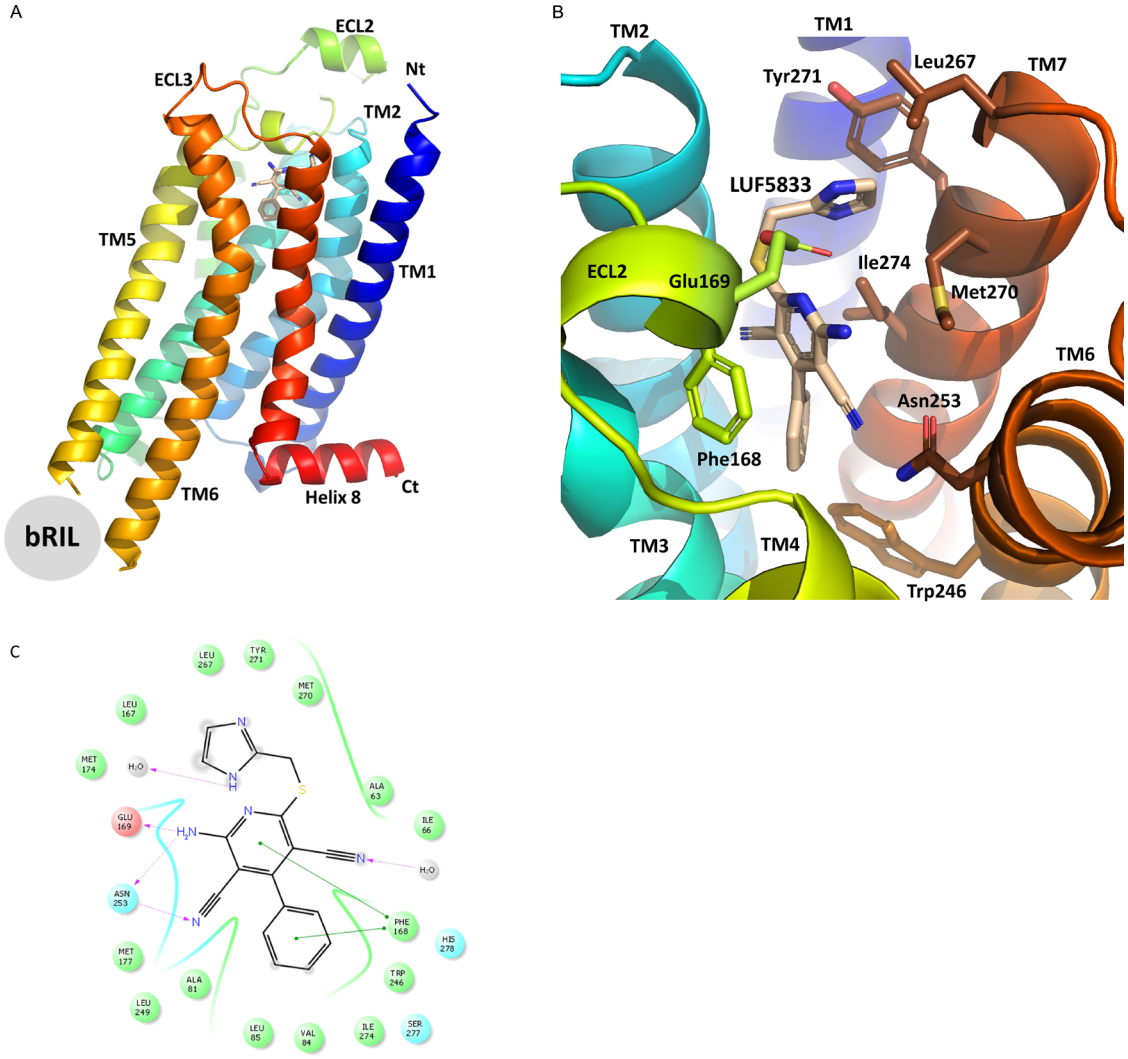

Figure 2. (A) Crystal structure of stabilized $hA_{2A}AR$-STaR2-bRIL in complex with partial agonist **8** (color-coded according to protein domains; TM: transmembrane domain; ECL: extracellular loop; Nt: N-terminus; Ct: C-terminus; bRIL structure omitted for clarity; compound **8** within TM cavity); (B) ligand binding site of **8** (LUF5833) surrounded by amino acids (three-letter code) within 4 Å distance; (C) two-dimensional representation of interacting amino acids and **8** docked into the $hA_{2A}AR$ crystal structure with all nine thermostabilizing mutations reverted to wild-type $hA_{2A}AR$, showing the ligand binding cavity within the 4 Å distance of **8** (green circle: hydrophobic; red circle: negatively charged; blue circle: polar; gray circle: water; gradient gray circle: solvent exposed).

thylimidazole (**7**) was synthesized by reducing the commercially available 2-imidazolecarboxaldehyde with sodium borohydride in absolute ethanol. Subsequent treatment with hydrobromic acid (33% in acetic acid) furnished the commonly used alkylating agent **7**.[11,21] Alkylation of intermediate **10** with agent **7** gave cyanopyrimidine **1** in a satisfactory 40% yield. The synthesis of **2** was started from the commercially available cyanuric chloride **11**. Grignard alkylation with phenylmagnesium bromide provided **12** in a relatively good yield of 52%. Amination was then performed using 1.0 equiv of concentrated aqueous ammonia to give crude **13**.[22] This was treated with an excess of sodium sulfide nonahydrate to furnish the crystalline intermediate **14**, which was alkylated using **7** to give the final compound **2**. Although compounds **1** and **3** are both cyanopyrimidine derivatives, the synthesis of compound **3**, in which the cyano group has an opposed topology, was slightly more laborious. Commercially available benzoyl acetonitrile (**15**) was treated with a strong base to form the enolate, which was reacted with carbon disulfide. The resulting dithiocarboxylic acid anions were reacted with iodomethane to form ketene dithioacetal **16**. The following cyclization, using guanidine hydrochloride and an excess base, provided the cyanopyrimidine scaffold.[23] Subsequent oxidation of the thioether gave sulfone **18**, which was subjected to a substitution-hydrolysis sequence using potassium thioacetate followed by a strong base.[24] The resulting free thiol (**19**) was then alkylated using **7** to provide the final compound **3** with a yield of 46%.

The synthetic routes toward the pyridine derivatives are shown in Scheme 2. The synthesis of compound **4** started with a Knoevenagel condensation between acetophenone and malononitrile.[25] The thus formed intermediate **21** was reacted with dimethyl cyanocarbonimidodithioate to establish the cyanopyridine core.[26] Similar to the synthesis route of compound **3**, treatment with *meta*-chloroperbenzoic acid (mCPBA) provided the sulfone (**23**), which was converted to free thiol **24**. Alkylation of the free thiol using **7** gave the final compound **4**. Similar to the synthesis of compound **2**, the synthesis of compound **5** started from a triple-halogen-substituted heteroaromatic system. Commercially available

https://doi.org/10.1021/acs.jmedchem.0c01856
J. Med. Chem. 2021, 64, 3827−3842

Scheme 1. Synthesis Route toward Pyrimidine and Triazine Derivatives 1−3[a]

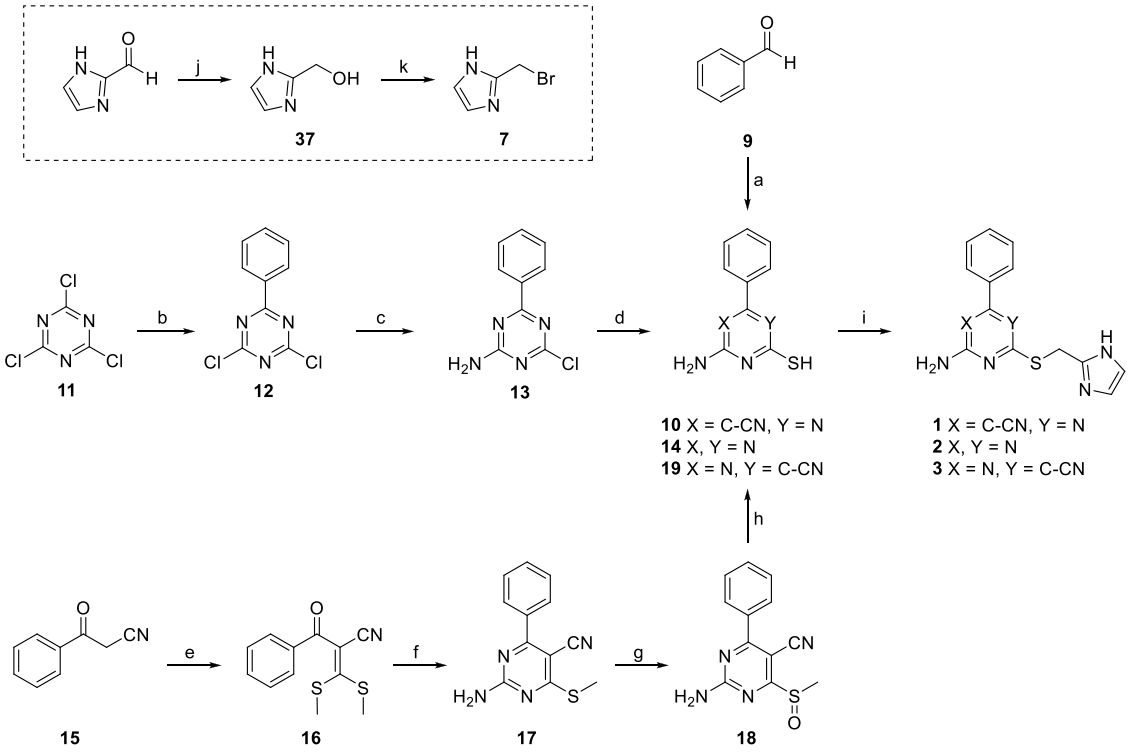

[a]Reagents and conditions: (a) malononitrile, thiourea, K_2CO_3, EtOH, reflux, 21% (for **10**); (b) *R*-phenylmagnesium bromide, dry THF, N_2, rt, 52%; (c) NH_3 (25%) in H_2O, CH_2Cl_2, rt, 66%; (d) $Na_2S{\cdot}9H_2O$, DMF, 80 °C, 28% (for **14**); (e) NaH, carbon disulfide, iodomethane, dry DMSO, N_2, rt, 82%; (f) guanidine hydrochloride, TEA, DMF, reflux, 42%; (g) mCPBA,CH_2Cl_2, rt, 66%; (h) potassium thioacetate, DMF, rt, 53% (for **19**); (i) **7**, Na_2CO_3, DMF, rt, 3−46%; (j) $NaBH_4$, absolute EtOH, rt, 75%; (k) 33% HBr in CH_3COOH, reflux, 65%.

2,6-dichloro-4-iodopyridine (**25**) was selectively alkylated on the 4-position using a Suzuki cross-coupling reaction to give intermediate **26** in quantitative yield.[27] Subsequent sequential nucleophilic aromatic substitution of the two chloro-groups using equimolar *tert*-butylthiol and *tert*-butyl carbamate, respectively, gave intermediate **28**.[28,29] Treatment with trifluoroacetic acid (TFA), followed by treatment with conc. HCl, yielded the deprotected intermediate **30** in two steps. It was later found that this deprotection sequence could also be performed in one step by directly using hydrochloric acid. The final compound **5** was obtained in a yield of 33% by alkylation of **30** with **7** using the same procedure as mentioned before. Last, toward compound **6**, commercially available ethylbenzoyl acetate (**31**) was reacted with 2-cyanoacetamide to give the cyanopyridine intermediate **32**, which was subjected to double chlorination using phosphorus oxychloride to yield the asymmetric cyanopyridine dichloride **33**.[30,31] In an initial attempt to directly substitute one of the chlorides, *tert*-butylthiol was added to intermediate **33**. However, even after varying the reaction temperature and substitution on the thiol, inseparable mixtures of 2-(*tert*-alkylthio)-6-chloro-substituted (desired compound), 6-(*tert*-alkylthio)-2-chloro-substituted, and disubstituted 2,6-bis(*tert*-alkylthio)-4-phenylnicotinonitrile were obtained. Instead, Buchwald−Hartwig amination using *tert*-butyl carbamate was attempted. Gratifyingly, using this procedure, intermediate **34** was obtained with the correct substitution and as a single product. Subsequent addition of *tert*-butylthiol followed by one-step deprotection of both protective groups using hydrochloric acid gave intermediate **36**, which was alkylated using the procedure mentioned previously to produce the final compound **6** in 8% yield.

Pharmacological Assessment of the Library of Compound 8 Derivatives. We first assessed the compounds' affinities for all adenosine receptor subtypes in radiolabeled antagonist[10] binding studies on cell membranes expressing the individual receptors (A_1: [^{3}H]DPCPX; A_{2A}: [^{3}H]ZM241385; A_{2B}: [^{3}H]PSB-603; A_3: [^{3}H]PSB-11). Single-point displacement assays at 1 μM on all four human adenosine receptor subtypes were performed as a preliminary assay for all compounds. Only compounds that showed greater than 50% radioligand displacement were evaluated in full-range concentration-dependent displacement assays to determine their affinities (Table 1 and Figure S4).

Of all compounds tested, the parent compound **8** displayed the highest affinity toward all human adenosine receptor subtypes, being slightly selective for the hA_1AR with a K_i value of 3 nM. Modification of **8** by changing one cyano group at the thiol side for a nitrogen atom in the pyridine core yielded compound **1** with a significant, 10−30 fold, decreased affinity toward all adenosine receptor subtypes. Changing the other cyano group in **8** in the same way at the other, "left-hand" side provided compound **3** with similar affinity to **8** on $hA_{2A}AR$ (K_i = 10 nM), while it showed approximately 25-fold lower affinity at hA_1AR and hA_3AR, rendering this compound the more selective derivative at $hA_{2A}R$. The non-nitrile triazine compound **2** displayed lower affinity at all adenosine receptor subtypes with minimal affinity toward $hA_{2B}AR$ (only 2% displacement of radioligand binding). The mono-cyano pyridine derivative **4** with structural resemblance to **1** displayed lower affinity than **1** on all adenosine receptor subtypes except $hA_{2B}AR$, where it had a K_i value of 370 nM, rendering it the more nonselective derivative over all four adenosine receptor

https://doi.org/10.1021/acs.jmedchem.0c01856
J. Med. Chem. 2021, 64, 3827−3842

Scheme 2. Synthesis Route toward Pyridine Derivatives 4−6[25a]

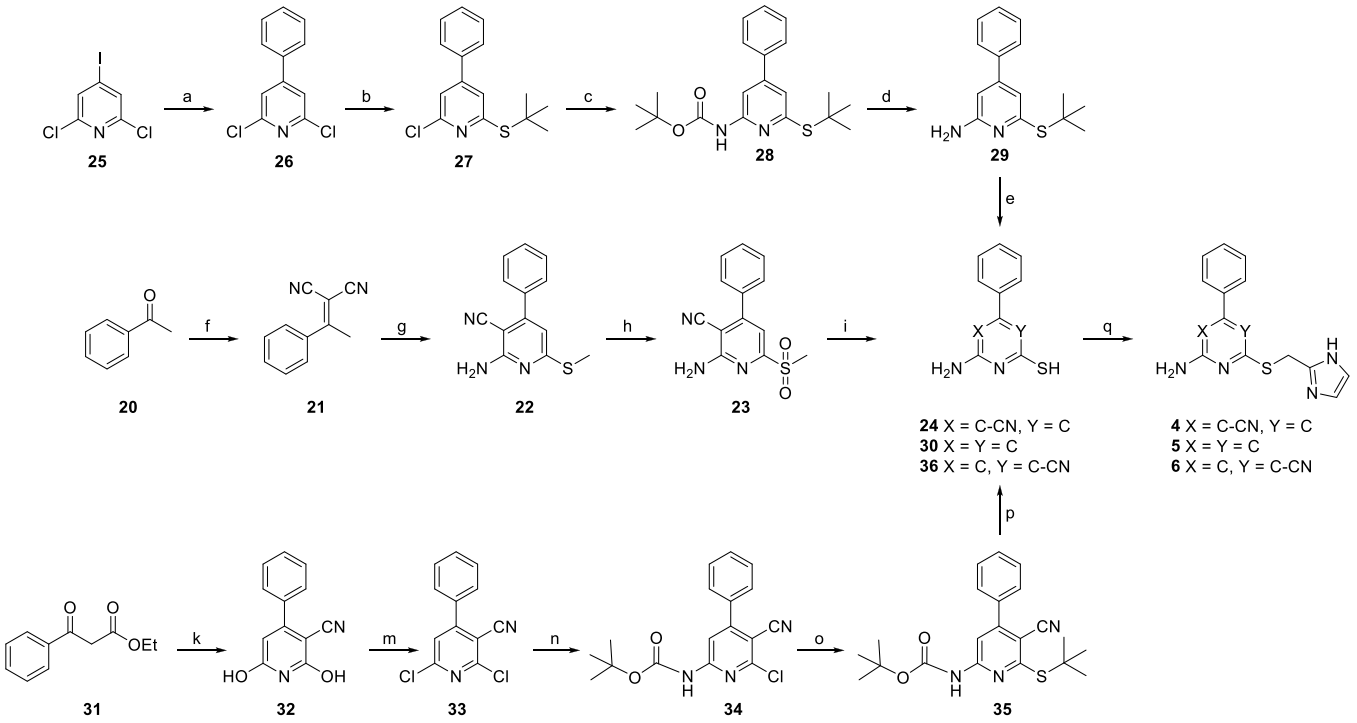

[a]Reagents and conditions: (a) phenylboronic acid pinacol esther, $Pd(PPh_3)Cl_2$, Na_2CO_3, H_2O/MeCN, N_2, 70 °C, 92%; (b) 2-methyl-propanethiol, Cs_2CO_3, DMF, 80 °C, quantitative yield; (c) $Pd(OAc)_2$, Xantphos, Cs_2CO_3, *t*-butyl carbamate, dry 1,4-dioxane, N_2, 110 °C, 27%; (d) TFA, CH_2Cl_2, reflux, 75%; (e) 37% HCl, 100 °C; (f) malononitrile, ammonium acetate, toluene, reflux in Dean−Stark apparatus, 70%; (g) (i) dimethyl cyanocarbonimidodithioate, K_2CO_3, DMF, rt, (ii) piperidine, 80 °C, 62%; (h) mCPBA,CH_2Cl_2, rt, 56%; (i) potassium thioacetate, DMF, rt, 61% (for **24**); (k) 2-cyanoacetamide, KOH, EtOH, reflux, 34%; (m) $POCl_3$ in an autoclave, 180 °C, 70%; (n) $Pd(OAc)_2$, Xantphos, Cs_2CO_3, *t*-butyl carbamate, dry 1,4-dioxane, N_2, 40 °C, 33%; (o) 2-methyl-propanethiol, Cs_2CO_3, DMF, 90 °C, 89%; (p) 37% HCl, 100 °C, 37% (for **36**); (q) **7**, $NaHCO_3$, DMF, rt, 8−57%.

Table 1. Affinities of 8 and Derivatives (1−6) in Radioligand Binding Assays on the Human Adenosine Receptors

	pK_i or % displacement[a]			
compound	A_1AR[b]	$A_{2A}AR$[c]	$A_{2B}AR$[d]	A_3AR[e]
8	8.52 ± 0.04	8.13 ± 0.05	7.40 ± 0.05	7.38 ± 0.01
1	7.07 ± 0.01	7.17 ± 0.08	51%[f]	6.46 ± 0.06
2	6.54 ± 0.05	6.25 ± 0.08	2%[f]	5.42 ± 0.06
3	7.16 ± 0.02	8.00 ± 0.05	50%[f]	5.94 ± 0.05
4	6.38 ± 0.06	6.42 ± 0.01	6.43 ± 0.03	5.57 ± 0.05
5	12%[g]	−17%[g]	−12%[f]	46%[g]
6	6.95 ± 0.08	5.99 ± 0.12	37%[f]	5.87 ± 0.10

[a]Data are expressed as mean ± SEM of three separate experiments each performed in duplicate, unless indicated otherwise. [b]Displacement of [^{3}H]DPCPX binding in CHO cells expressing hA_1AR. [c]Displacement of [^{3}H]ZM241385 binding in HEK293 cells expressing $hA_{2A}AR$. [d]Displacement of [^{3}H]PSB-603 binding in CHO cells expressing $hA_{2B}AR$. [e]Displacement of [^{3}H]PSB-11 binding in CHO cells expressing hA_3AR. [f]Percent displacement (n = 2) of specific [^{3}H]PSB-603 binding in CHO cells expressing $hA_{2B}AR$ at 1 μM ligand concentrations. [g]Percent displacement (n = 2) of specific radioligand binding at 10 μM ligand concentrations.

subtypes. The mono-cyano pyridine derivative **6** with the same cyano position as in pyrimidine **3** showed a significant, 100-fold lower affinity to $hA_{2A}AR$ compared to **3**, although it had similar affinity to the other subtypes. Pyridine **5**, lacking both cyano groups, was almost devoid of affinity at all adenosine receptor subtypes, as it showed no or negligible displacement of radioligand binding in the preliminary single-concentration assays (1 μM). Apparently, the number of nitrogen atoms in or around the scaffold is an important determinant of receptor binding, especially for $hA_{2A}AR$.

Next, we examined the compounds' efficacy/intrinsic activity in a label-free impedance-based assay on cells expressing $hA_{2A}AR$. As the parent compound **8** had been identified as a partial agonist,[11,12] we sought to characterize the new derivatives for their functional behavior along the agonist/antagonist spectrum. Intrinsic activities of **8** and its derivatives at $hA_{2A}AR$ were assessed using a label-free whole-cell assay with a real-time cell analysis (RTCA) system by measuring the flow of electrons transmitted between two gold electrodes at the bottom of a well in a 96-well plate. Upon receptor activation, the HEK293$hA_{2A}R$ cell morphology changes and covers more of the electrodes, which impedes the electron flow. The impedance produced is displayed as a unit-less number, the so-called cell index (CI).[32] A reference full agonist of $hA_{2A}AR$, ribose-containing CGS21680, was used to define the highest CI observed, and the peak values obtained were used to determine EC_{50} values. Concentration−response curves of CGS21680 and the compounds in the library are displayed in Figure 3. In this study, the parent compound **8** showed a lower potency than CGS21680 and acted as a partial agonist of the receptor, with an intrinsic activity (E_{max} value) of 66 ± 5% (Table 2). A similar observation had been reported in a previous study by Beukers *et al.*,[11] focusing on cAMP production as a signaling readout.

https://doi.org/10.1021/acs.jmedchem.0c01856
J. Med. Chem. 2021, 64, 3827−3842

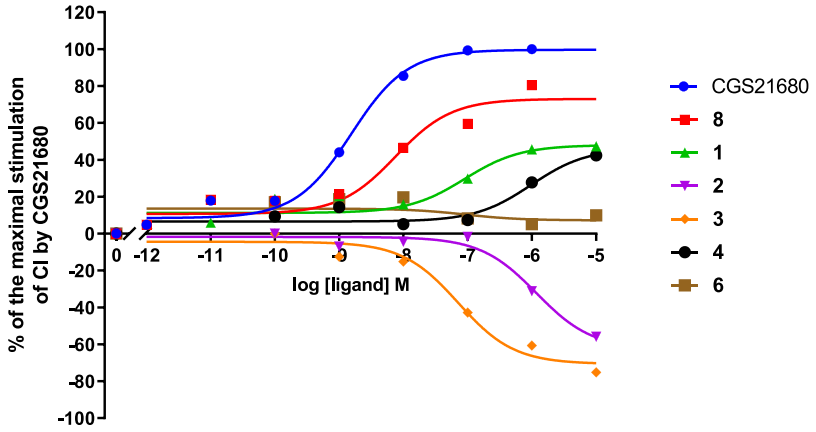

Figure 3. Concentration–response curves for CGS21680 and nonriboside compounds at HEK293hA_{2A}R derived from the peak analysis of cell index (CI) changes obtained in the xCELLigence RTCA system. The cellular responses were normalized and shown as % of the maximal CI by 1 μM CGS21680. Representative graphs from one experiment performed in duplicate.

Table 2. Compound Potency and Intrinsic Activity Derived from the Label-Free Whole-Cell Assay Performed on HEK293-hA_{2A}R Cells[a]

compound	pEC_{50}	E_{max}, %
CGS21680	8.85 ± 0.08	100 ± 2
8	8.01 ± 0.22	66 ± 5
1	6.57 ± 0.37	41 ± 5
2	6.09 ± 0.23	−48 ± 5
3	7.35 ± 0.28	−50 ± 5
4	5.78 ± 0.38	37 ± 7
6	N.D.	N.D.

[a]Data are shown as mean ± S.E.M. of three independent experiments performed in duplicate. Log potency (pEC_{50}) and efficacy (E_{max}) were calculated from concentration–response curves derived from the peak analysis of CI changes. N.D., not determined.

Various responses were shown by the nonriboside derivatives. The pyrimidine compound **1** behaved as a partial agonist as well (E_{max} = 41 ± 5%), although it had lower potency than **8** (pEC_{50} of 6.57 ± 0.37 vs 8.01 ± 0.22). The pyridine derivative **4** was a partial agonist too (E_{max} = 37 ± 7%) but with the lowest measurable potency in the series (pEC_{50} = 5.78 ± 0.38). Remarkably, compound **3**, the derivative with the highest selectivity for hA_{2A}AR, had an opposite activity compared to **8**. Figure 3 shows that this cyanopyrimidine compound acted as an inverse agonist at the receptor (E_{max} = −50 ± 5%) with a potency quite comparable to **8** (pEC_{50} = 7.35 ± 0.28). The absence of both cyano groups in the triazine compound **2** also led to inverse agonism at hA_{2A}AR with similar efficacy (−48 ± 5%) to **3**, albeit with significantly lower potency (pEC_{50} = 6.09 ± 0.23 vs 7.35 ± 0.28). Compound **6** did not show any measurable degree of intrinsic activity, as it neither activated nor inactivated the receptor (Figure 3). These results show that modification/deletion of the cyano groups alters the functional characteristics of the compounds. Keeping the cyano group at the amino, "left-hand" side maintained agonism, while the absence of this group abolished this feature, resulting in inverse agonism for **2** and **3** and, possibly, neutral antagonism for **6**.

Molecular Modeling. Intrigued by the findings in the pharmacological experiments, we decided to perform induced-fit docking studies of compounds **1** and **3**, the two compounds with the most obvious differences in receptor activation patterns while having appreciable affinity for the adenosine A_{2A} receptor. To prepare the receptor structure for this analysis, the bRIL fusion partner was removed from the crystal structure and the third intracellular loop (ICL3) was implemented again.[33] Mutated amino acids used to thermostabilize the structure in the crystallization process, such as M1P, A54L, T88A, R107A, K122A, N154A, L235A, and V239A, were changed back to the wild-type amino acids. Missing water molecules were retrieved from a previous high-resolution crystal structure (PDB ID: 4EIY)[2] to provide stability of the receptor–ligand interaction in the docking simulation. First, as a control experiment, compound **8** was docked into this wild-type hA_{2A}AR model. Induced flexible docking allowed the imidazole moiety to adopt slightly different positions, not surprisingly in view of its orientation toward the more flexible extracellular loops. The dicyanopyridine scaffold, however, did hardly move (Figure S5). Next, compounds **1** and **3** were flexibly docked[34] into the binding pocket with the binding pose of **8** as a reference (Figures 4–6, respectively). The partial agonist **1** showed a similar binding pose as **8** after convergence of the docking procedure, with two hydrogen bonds with $Asn253^{6.55}$, one hydrogen bond with $Glu169^{ECL2}$, a π–π stacking interaction with $Phe168^{5.29}$, and its phenyl moiety surrounded by $Ser277^{7.42}$ and $His278^{7.43}$ (Figures 4 and 6). The inverse agonist **3** took a slightly different pose due to the absence of the cyano substituent on the "left-hand" side of the molecule. The ligand moved closer to $Asn253^{6.55}$ as to maintain hydrogen bonding, now to the nitrogen atom in the ligand's core. As a result, it also forms two hydrogen bonds with $Asn253^{6.55}$, one hydrogen bond with $Glu169^{ECL2}$, and a π–π stacking interaction between its pyrimidine core and $Phe168^{5.29}$. However, this movement also caused a shift of the phenyl moiety away from $Ser277^{7.42}$ and $His278^{7.43}$, bringing this moiety closer to $His250^{6.52}$ (Figures 5 and 6). A similar alignment is also present in the binding pocket of antagonist/inverse agonist ZM241385. Its furan ring forms a π–π stacking interaction with $His250^{6.52}$ (Figure S2A).

DISCUSSION AND CONCLUSIONS

The ligand binding pocket of **8** encompasses amino acids that have been subjected to a mutagenesis study by Lane *et al.* in which the reference agonist CGS21680 and LUF5834 (Figure 1), a close analogue of **8**, were compared.[16] In fact, within the scope of the present study, we also attempted to obtain a

https://doi.org/10.1021/acs.jmedchem.0c01856
J. Med. Chem. 2021, 64, 3827–3842

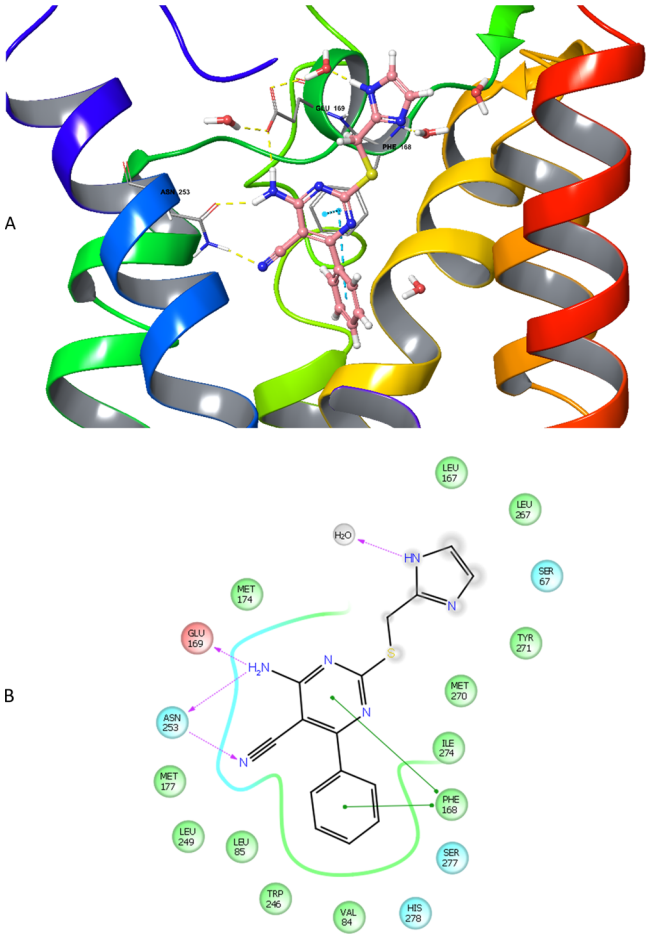

Figure 4. (A) Proposed binding mode of compound **1** in the $hA_{2A}AR$ crystal structure with all nine thermostabilizing mutations reverted to wild-type $hA_{2A}AR$, obtained by induced-fit docking. It shows the interactions formed between **1** and the receptor, in particular three hydrogen bond interactions with $Asn253^{6.55}$ and $Glu169^{5.30}$, and two $\pi-\pi$ stacking interactions with $Phe168^{5.29}$. A part of helix 7 was omitted for better visualization. (B) Two-dimensional representation of the interaction between **1** and $hA_{2A}AR$ in the ligand binding cavity within a 4 Å distance (green circle: hydrophobic; red circle: negatively charged; blue circle: polar; gray circle: water; gradient gray circle: solvent exposed). The phenyl moiety is surrounded by $Ser277^{7.42}$ and $His278^{7.43}$, key residues in receptor activation.

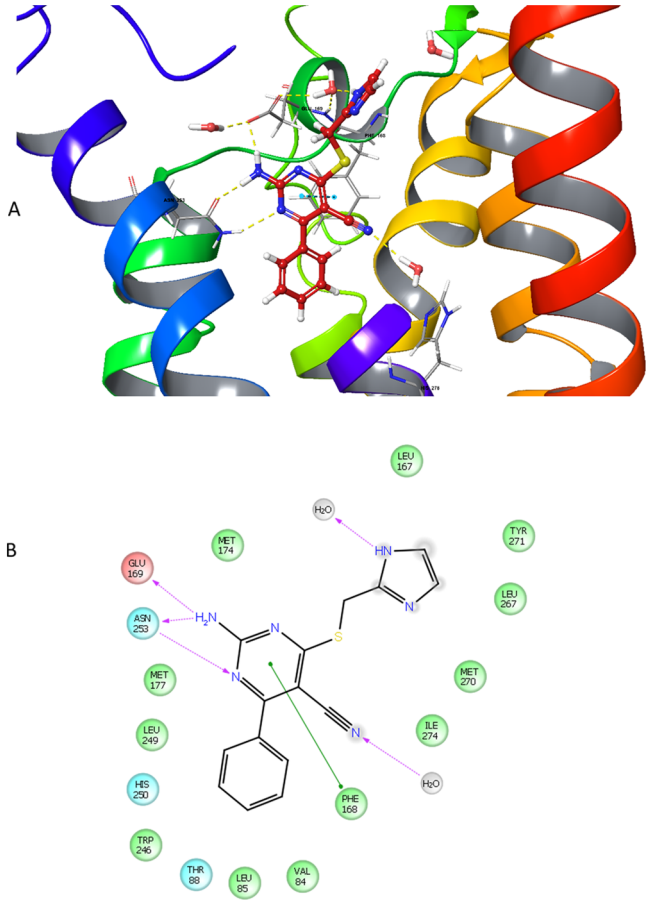

Figure 5. (A) Proposed binding mode of compound **3** in the $hA_{2A}AR$ crystal structure with all nine thermostabilizing mutations reverted to wild-type $hA_{2A}AR$, obtained by induced-fit docking. Compared to Figure 4 (compound **1**), the hydrogen bond interaction between the nitrogen atom in the pyrimidine ring and $Asn253^{6.55}$ causes a shift of **3**'s position in the binding cavity. A part of helix 7 was omitted for better visualization. (B) Two-dimensional representation of the interaction between **3** and $hA_{2A}AR$ in the ligand binding cavity within a 4 Å distance (green circle: hydrophobic; red circle: negatively charged; blue circle: polar; gray circle: water; gradient gray circle: solvent exposed). Most key interactions for binding to the receptor are maintained, but the phenyl moiety is moved away from $Ser277^{7.42}$ and $His278^{7.43}$.

receptor crystal structure with LUF5834 but were unsuccessful. The authors performed cAMP measurements to demonstrate that the potencies of both CGS21680 and LUF5834 were dramatically (>100-fold) reduced in the $Phe168^{5.29}$ alanine mutant, in accordance with the pivotal role this amino acid plays in coordinating the scaffold and phenyl substituent of **8** in the crystal structure. The $Asn253^{6.55}$ alanine mutation negatively affected CGS2160 potency and LUF5834 intrinsic activity, with the latter losing its partial agonist activity and turning into an antagonist. The Ala mutant of $Glu169^{EL2}$ on the contrary slightly increased the potency and intrinsic activity of LUF5834 with no effect on CGS21680. This amino acid has been shown to interact with a histidine ($His264^{6.66}$) residue to form a lid above the binding pocket of the receptor, affecting the residence time of AR ligands.[13] Alanine mutation of $Ser277^{7.42}$, as present in the crystal structure, reduced the potency of CGS21680 by two orders of magnitude, while LUF5834's potency and affinity increased somewhat and the compound turned into a full agonist.

Rather than reiterating this mutagenesis study to include **8**, we decided to synthesize and test six derivatives of the compound for a further analysis of its agonistic characteristics. The decoration of the scaffold was altered in a one-by-one step fashion to compare the effect of relatively minor changes on both potency and intrinsic activity. These structural alterations caused changes in affinity, as assessed on all four adenosine receptor subtypes through radioligand binding studies. All compounds were less active than **8**, in particular compound **5**, bearing the pyridine scaffold without cyano substituents. Interestingly, compound **3** was the most selective for $hA_{2A}AR$; it kept its affinity on this receptor subtype, while its affinity for the other adenosine receptor subtypes dropped substantially (Table 1).

We then examined the functional characteristics of the compounds in label-free functional experiments on intact HEK293 cells overexpressing $hA_{2A}AR$. We had reported

https://doi.org/10.1021/acs.jmedchem.0c01856
J. Med. Chem. 2021, 64, 3827−3842

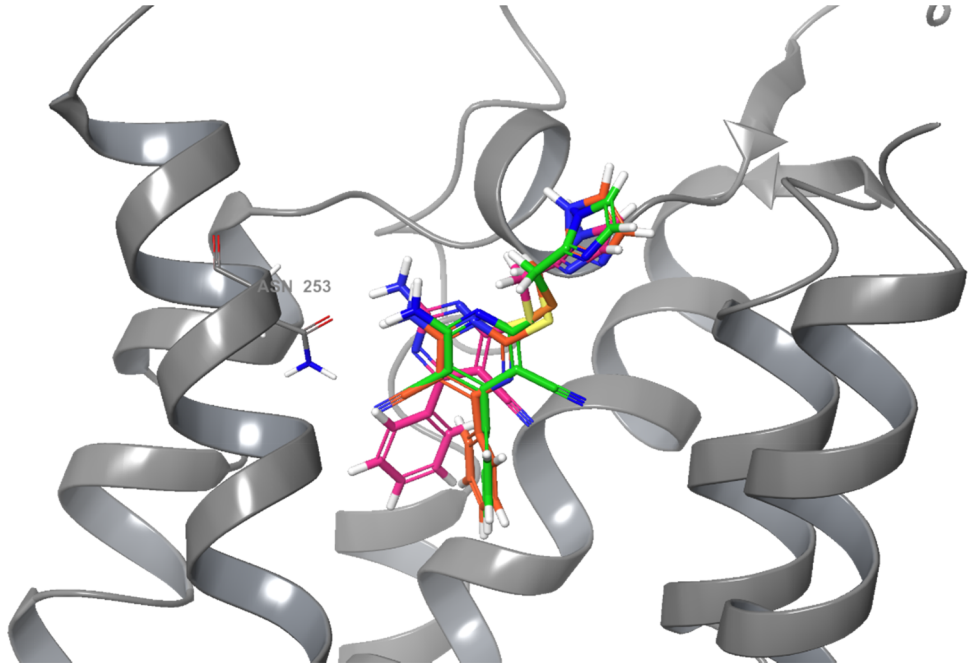

Figure 6. Superimposition of compounds **1** (orange), **3** (pink), and **8** (green) in the $hA_{2A}AR$ crystal structure with all nine thermostabilizing mutations reverted to wild-type $hA_{2A}AR$, obtained by induced-fit docking. For reasons of clarity, only five helices and the amino acid Asn253$^{6.55}$ are shown.

previously that the endogenous expression of $hA_{2B}AR$ on these cells does not compromise the functional evaluation of $hA_{2A}AR$ occupancy.[16] Hence, we were able to record the pEC_{50} values of all compounds in this cell system (Table 2 and Figure 4) and compared these with the radioligand binding data. The pK_i and pEC_{50} values were strongly correlated ($r^2 = 0.91$, $P = 0.01$, Figure S6) yet another indication of the unequivocal involvement of $hA_{2A}AR$. It also suggests there is no or negligible receptor reserve, in line with the partial nature of the compounds' efficacy.

We were quite surprised to record huge changes in intrinsic activity. Here, some of the compounds (**2** and **3**) were turned into inverse agonists instead of (partial) agonists. Only compounds **1** and **4**, both retaining the cyano substituent on the "left-hand" side of the molecule, kept the partial agonist profile as in **8**. Induced-fit docking studies helped interpret our pharmacological findings. Subtle ligand movements in the binding pocket carried some ligands away from "agonistic" amino acids to negate their activation potential, while other ligands kept a partial agonistic profile. These ligand movements may also be dependent on the presence of explicit water molecules. In the $hA_{2A}AR$-ZM241385 crystal structure, three water molecules occupy a region next to the furan ring of ZM241385,[2,3] which is taken by the riboside moiety in an $hA_{2A}AR$-agonist structure.[35] It is entirely plausible that **8** and derivatives take intermediate positions with varying amounts of water molecules, reflecting their antagonistic vs agonistic nature. In a previous study focusing on the hA_1AR, we had synthesized a series of quite different monocyanopyrimidines but also with the cyano substituent on either the "left hand" or "right hand" side of the scaffold.[36] These compounds were all inverse agonists, however, suggesting that depending on the hAR subtype, subtle changes at various parts of these molecules can alter the activation profile dramatically and differently.

In conclusion, in this study, we elucidated the structure of the adenosine A_{2A} receptor bound to a chemically distinct partial agonist, compound **8**. The interaction profile between the ligand and the receptor included amino acids that had been shown to be involved in receptor activation in earlier, e.g., mutagenesis studies. The synthesis and molecular docking of a series of derivatives of the partial agonist allowed us to further investigate the requirements for receptor activation. With this newly solved structure, we significantly expand the repertoire of A_{2A} receptor structures, allowing a more elaborate analysis of the ligand binding pocket than in any other GPCR.

EXPERIMENTAL SECTION

Crystal Structure Determination. *A_{2A}-Star2 bRIL Construct.* The A_{2A}-StaR2 construct consists of nine thermostabilizing mutations: A54L$^{2.52}$, T88A$^{3.36}$, R107A$^{3.55}$, K122A$^{4.43}$, N154A, L202A$^{5.63}$, L235A$^{6.37}$, V239A$^{6.41}$, and S277A$^{7.42}$. The first three amino acids at the N-terminus were deleted and the protein had a C-terminal truncation after L315 where 3 additional alanines and 10 histidines were added. The apocytochrome b 562 RIL (bRIL) was inserted into the third intracellular loop (ICL3) between residues L208 and G218.

Expression. The A_{2A}-StaR2-bRIL was expressed using the baculovirus system. Tni PRO cells were grown in suspension in flasks up to a maximum volume of 500 mL in 2 L roller bottles at 27 °C with shaking. Cells were grown in ESF921 (Expression Systems) medium supplemented with 5% (v/v) FBS and 1% (v/v) penicillin/streptomycin. Cells were infected at a density of 2.6×10^6 cells/mL with recombinant virus at an approximate multiplicity of infection of 1. Cells were harvested by centrifugation 48 h post infection.

Membranes were prepared from a pellet of 2 L cells resuspended in 40 mM Tris−HCl (pH 7.6), 1 mM EDTA, and Complete EDTA-free protease inhibitor cocktail tablets (Roche). Cells were disrupted through a microfluidizer (processor M-110L Pneumatic, Microfluidics) cooled down with ice (lysis pressure, ∼15,000 psi) and membranes were pelleted by centrifugation at 200,000*g* for 50 min. Membranes were washed with 40 mM Tris−HCl (pH 7.6), 1 M NaCl, and Complete EDTA-free protease inhibitor cocktail tablets

https://doi.org/10.1021/acs.jmedchem.0c01856
J. Med. Chem. 2021, 64, 3827−3842

and centrifuged at 200,000*g* for 50 min. After removal of the supernatant, membranes were resuspended in 50 mL with 40 mM Tris−HCl (pH 7.6) and Complete EDTA-free protease inhibitor cocktail tablets and frozen at −80 °C.

Purification and Lipidic Cubic Phase Crystallization. Cells from 2 L cultures were resuspended and disrupted using a microfluidizer (Processor M-110L Pneumatic, Microfluidics). Membranes pelleted by ultracentrifugation were subjected to a high-salt wash in a buffer containing 1 M NaCl before being resuspended in 50 mL of 40 mM Tris (pH 7.6) supplemented with Complete EDTA-free protease inhibitor cocktail tablets and stored at −80 °C until further use. Membranes were thawed, resuspended in a total volume of 150 mL, and incubated with 3 mM theophylline (Sigma-Aldrich) for 2 h at room temperature. Membranes were then solubilized by addition of 1.5% *n*-decyl-*β*-D-maltopyranoside (DM, Anatrace) and incubation for 2 h at 4 °C, followed by centrifugation at 145000*g* for 60 min to harvest a solubilized material. The solubilized material was applied to a 5 mL Ni-NTA (nickel-nitrilotriacetic acid) Superflow cartridge (Qiagen) and the protein was eluted with a buffer containing 1 mM theophylline. Collected fractions were pooled, concentrated, and applied to a Superdex200 size exclusion column (GE Healthcare). Fractions containing the protein were then concentrated to ∼35 mg/mL and subjected to an ultracentrifugation at 436,000*g* prior to crystallization. Protein concentrations were measured using the detergent compatible (DC) protein assay (Bio-Rad).

The A_{2A}-StaR2-bRIL was crystallized first in complex with theophylline in the lipidic cubic phase at 20 °C. The final protein/lipid ratio was 40:60 (w/w), and 40 nL of boli was dispensed using a Mosquito LCP crystallization robot (TTP Labtech) and overlaid with 800 nL of precipitant solution. Crystals grew within 2 weeks in 0.1 M trisodium citrate (pH 5.3−5.4), 0.05 M sodium thiocyanate, 29−32% PEG400, 2% (v/v) 2,5-hexanediol, and 0.5 mM theophylline. Then, incisions were made into the Laminex cover over base wells containing crystals, and wells were flooded with 10 *μ*L of mother liquor supplemented by compound **8** (1 mM). Flooded wells were then resealed and plates were incubated for 24 h at 20 °C. Single crystals were mounted in LithoLoops (Molecular Dimensions Ltd.) and flash-frozen in liquid nitrogen without the addition of further cryoprotectant.

Data Collection and Structure Solution. X-ray diffraction data (0.25°/frame; ∼500 frames) were collected on an Eiger 16M detector at beamline X06SA (Swiss Light Source) in a single swipe from one crystal. Integration was carried out using XDS[37] and scaled using aP scale[38] (Global Phasing, Cambridge, U.K.). The structure of the A_{2A}-StaR2-bRIL complex with compound **8** was solved by molecular replacement (MR) with Phaser[39] within the CCP4 interface using the previously reported A_{2A}-StaR2-bRIL-theophylline complex structure as the search model (PDB code: 5MZJ). Model refinement was performed initially using phenix.refine[40] and then using BUSTER[41] (Global Phasing), including TLS refinement for two groups corresponding to the receptor and bRIL562, respectively. The crystallographic data reduction and refinement statistics are presented in Table 3.

Chemistry. All solvents and reagents were of analytical grade and purchased from commercial sources. Demineralized water was simply referred to as H_2O and used in all cases, unless stated otherwise (i.e., brine). Thin-layer chromatography (TLC), aluminum-coated Merck silica gel F254 plates were used to monitor the progression of the reactions. The ^{1}H NMR spectra were recorded on a Bruker AV400 liquid spectrometer (^{1}H NMR, 400 MHz; ^{13}C NMR, 100 MHz) at ambient temperature. Chemical shifts are reported in parts per million (ppm), designated by *δ* and downfield to the internal standard tetramethylsilane (TMS) in $CDCl_3$. Coupling constants are reported in Hz and designated as *J*. The analytical purity of the final compounds was determined by high-performance liquid chromatography (HPLC) with a Phenomenex Gemini 3 *μ*m C18 110 Å column (50 × 4.6 mm, 3 *μ*m), measuring UV absorbance at 254 nm. Sample preparation and HPLC method were as follows: 0.3−1.0 mg of compound was dissolved in 1 mL of a 1:1:1 mixture of MeCN/H_2O/*t*BuOH and eluted from the column within 15 min at a flow rate of 1.3 mL/min with a three-component system of H_2O/MeCN/1% TFA in H_2O. The elution method was set up as follows: in a 1−4 min isocratic system of H_2O/MeCN/1% TFA in H_2O, 80:10:10, from the 4th min, a gradient was applied from 80:10:10 to 0:90:10 within 9 min, followed by 1 min of equilibration at 0:90:10 and 1 min at 80:10:10. All final compounds showed a single peak at the designated retention time and were thus considered at least 95% pure. Liquid chromatography−mass spectrometry (LC−MS) analyses were performed on a Thermo Finnigan Surveyor−LCQ Advantage Max LC−MS system, Shimadzu LCMS-2020 system, and Phenomenex Gemini C18 110A columns (50 × 4.6 mm, 3 *μ*m; 50 × 3 mm, 3 *μ*m). The sample preparation was the same as for HPLC analysis. The compounds were eluted from the column within 15 min after injection, with a three-component system of H_2O/MeCN + 0.1% FA, while decreasing the polarity of the solvent mixture in time from 90:10 to 10:90. Purification by column chromatography was achieved by use of Grace Davison Davisil silica column material (LC60A 30−200 micron). Solutions were concentrated using a Heidolph Laborota W8 2000 efficient rotary evaporation apparatus. All reactions in the synthetic routes were performed without a nitrogen atmosphere, unless stated otherwise.

*(1H-Imidazol-2-yl)methanol (**37**).*[11] To a suspension of $NaBH_4$ (0.787 g, 20.8 mmol, 2.0 equiv) in absolute EtOH (15 mL) was added commercially available 1*H*-imidazole-2-carbaldehyde (1 g, 10.4 mmol, 1.0 equiv) portion-wise. The mixture was stirred at room temperature for 3 h. After the completion of the reaction, the mixture was quenched with water and concentrated *in vacuo*. The crude compound was purified by flash column chromatography (10% MeOH in $CHCl_3$) to obtain **37** as a pale yellow solid (769 mg, 7.85 mmol, 75%). ^{1}H NMR (400 MHz, MeOD): *δ* 6.97 (s, 2H, imidazoyl), 4.61 (s, 2H, CH_2).

Table 3. Data Collection and Refinement Statistics

	A_{2A}-LUF5833 (compound **8**)
data collection	
number of crystals	1
space group	$C222_1$
cell dimensions	
a, *b*, *c* (Å)	39.54, 181.03, 140.85
α, *β*, *γ* (°)	90, 90, 90
resolution (Å)	43.09−3.12 (3.31−3.12)[a]
no. of reflections	7990 (399)[a]
R_{pim}	0.134 (0.934)[a]
$I/\sigma(I)$	5.2 (1.1)[a]
$CC_{1/2}$	0.992 (0.309)[a]
completeness (%)	
spherical	84.5 (26.3)[a]
ellipsoidal	87.2 (32.5)[a]
redundancy	3.9 (4.0)[a]
refinement	
resolution (Å)	43.09−3.12
R_{work}/R_{free}	0.223/0.254
no. of atoms	
protein	2937
ligand	24
other	69
B factors	
protein	77.21
ligand	62.56
other	67.69
r.m.s. deviations	
bond lengths (Å)	0.007
bond angles (°)	0.81

[a]Values in parentheses are for the highest-resolution shell.

https://doi.org/10.1021/acs.jmedchem.0c01856
J. Med. Chem. 2021, 64, 3827−3842

2-(Bromomethyl)-1H-imidazole hydrobromide (7).[11] A suspension of **37** (0.55 g, 5.6 mmol) in HBr 33% (w/v) acetic acid solution (10 mL) was heated at 100 °C for 5 h. The mixture was concentrated *in vacuo* and treated with 25% PET in diethyl ether. The suspended solid was collected by filtration and dried to give **7** as a pale brown solid (885 mg, 3.66 mmol, 65%). ^{1}H NMR (400 MHz, MeOD): δ 7.60 (s, 2H, imidazolyl), 4.82 (s, 2H, CH_2). HNMR is consistent with the reported literature data.

4-Amino-2-sulfanyl-6-phenylpyrimidine-5-carbonitrile (10).[20] To malononitrile (0.99 g, 15 mmol, 1.0 equiv) dissolved in ethanol (7.5 mL) were added benzaldehyde (1.528 mL, 15 mmol, 1.0 equiv), thiourea (1.14 g, 15 mmol, 1.0 equiv), and K_2CO_3 (2.07 g, 15 mmol, 1.0 equiv). The mixture was stirred at reflux for 5 h. Upon the completion of the reaction, the precipitate formed in the mixture was filtered and then stirred with warm water (50 °C). The filtrate was acidified with acetic acid to pH below 7. The precipitate formed was filtrated and dried *in vacuo* to obtain **10** as a white solid (716 mg, 3.14 mmol, 21%). ^{1}H NMR (400 MHz, DMSO): δ 13.07 (br s, 1H, SH), 8.45 (br s, 1H, 0.5 NH_2), 7.93 (br s, 1H, 0.5 NH_2), 7.68 (d, J = 6.8 Hz, 2H, Ph), 7.63−7.53 (m, 3H, Ph).

2-(1H-Imidazol-2-yl)methylthio-4-amino-6-phenylpyrimidine-5-carbonitrile (1). Alkylation was performed according to previously reported procedures.[11] To a solution of free thiol **10** (0.684 g, 3 mmol, 1.0 equiv) in DMF (12 mL) were added 2-bromomethylimidazole **7** (0.483 g, 3 mmol, 1.0 equiv) and Na_2CO_3 (0.318 g, 3 mmol, 1.0 equiv). The reaction was stirred at 50 °C for 4 h. Water (60 mL) was added to force the crude product to precipitate, which was collected by filtration. The precipitate was washed with DMF (6 mL) and EtOAc (6 mL), and water (30 mL) was added to cause precipitation, which was filtered and dried *in vacuo* to obtain the desired product as a white powder (370 mg; 1.20 mmol; yield, 40%). Mp 237 °C. ^{1}H NMR (850 MHz, DMSO): δ 11.85 (br s, 1H, NH), 8.30 (br s, 1H, imidazolyl), 7.86−7.84 (m, 2H, Ph), 7.80 (br s, 1H, imidazolyl), 7.58 (tt, J = 7.6, 1.7 Hz, 1H, Ph), 7.54 (tt, J = 6.8, 1.7 Hz, 2H, Ph), 7.10−6.80 (m, 2H, NH_2), 4.43 (s, 2H, CH_2). MS (ESI): calcd for $C_{15}H_{12}N_6S$ $[M + H]^+$, 309.08; found: 309.00. HPLC: 3.107 min; purity: 99%.

2,4-Dichloro-6-phenyl-1,3,5-triazine (12).[42] To a stirred suspension of commercially available cyanuric chloride **11** (0.5 g, 2.71 mmol, 1.0 equiv) in dry THF (20 mL) at 0 °C under a nitrogen atmosphere was added a 3 M solution of phenylmagnesium bromide (0.993 mL, 2.98 mmol, 1.1 equiv) in THF (10 mL) dropwise (over 30 min). The reaction mixture was stirred at room temperature for 6 h. Upon the completion of the reaction (monitored by TLC), the mixture was treated with 10% aqueous HCl (50 mL) and extracted with EtOAc (40 mL × 3). The combined organic layer was washed with water (30 mL), dried on $MgSO_4$, and evaporated under reduced pressure to give the intermediate as a brown solid (318 mg, 1.42 mmol, 52%). The crude product was used for the next reaction without further purification. ^{1}H NMR (400 MHz, $CDCl_3$) δ 8.50 (dd, J = 8.0, 1.6 Hz, 2H, Ph), 7.66 (tt, J = 7.6, 1.2 Hz, 1H, Ph), 7.54 (t, J = 8.0 Hz, 2H, Ph).

4-Chloro-6-phenyl-1,3,5-triazine-2-amine (13).[43] Aqueous ammonia (25%) was added dropwise (0.1 mL, 1.327 mmol, 1.0 equiv) to a stirred solution of **12** (0.3 g, 1.327 mmol, 1.0 equiv) in CH_2Cl_2 (5 mL). The resulting mixture was stirred at room temperature for 8 h. The reaction progress was monitored by TLC. The precipitate formed was filtered, rinsed with CH_2Cl_2 (30 mL), and dried under reduced pressure, affording a pale orange solid of **13** (180 mg, 0.87 mmol, 66%). The compound was used in the next reaction without further purification. ^{1}H NMR (400 MHz, $CDCl_3$) δ 8.40 (d, J = 8.0, 1.6 Hz, 2H, Ph), 7.57 (tt, J = 7.6, 1.6 Hz, 1H, Ph), 7.51 (t, J = 8.0 Hz, 2H, Ph), 5.71 (br s, 2H, NH_2). MS (ESI) calcd for $C_9H_7ClN_4$ $[M + H]^+$: 207.04; found, 207.10.

4-Amino-6-phenyl-1,3,5-triazine-2-thiol (14).[44] A suspension of **13** (0.68 g, 3.29 mmol, 1.0 equiv) and sodium sulfide nonahydrate (1.185 g, 4.93 mmol, 1.5 equiv) in DMF (3 mL) was stirred at 80 °C for 3 h. The reaction progress was monitored by TLC. DMF was evaporated under reduced pressure at 80 °C. The resulting residue was treated carefully with HCl in EtOAc (10 mL). The suspended solid was collected by filtration and extracted with boiling EtOH (20 mL × 5). The collected organic layers were concentrated *in vacuo* and washed with warm DCM (15 mL × 3) to afford a pale yellow solid (190 mg, 0.92 mmol, 28%). ^{1}H NMR (400 MHz, DMSO) δ 12.84 (br s, 1H, SH), 8.22 (d, J = 7.6 Hz, 2H, Ph), 8.20 (br s, 1H, 0.5 NH_2), 7.77 (br s, 1H, 0.5 NH_2), 7.59 (t, J = 7.6 Hz, 1H, Ph), 7.51 (t, J = 8.0 Hz, 2H, Ph). MS (ESI) calcd for $C_9H_8N_4S$ $[M + H]^+$, 205.05; found, 205.10.

4-(1H-Imidazol-2-yl)methylthio-6-phenyl-1,3,5-triazin-2-amine (2). Similar procedure as synthesis of **1** using **14** (0.148 g, 0.725 mmol, 1.0 equiv) as a starting material. The final compound **2** was obtained as a white solid (7 mg; 0.02 mmol; yield, 3%). Mp 209 °C. ^{1}H NMR (400 MHz, MeOD): δ 8.34 (dd, J = 8.4, 1.2 Hz, 2H, Ph), 7.53 (tt, J = 7.6, 1.2 Hz, 1H, Ph), 7.45 (t, J = 7.6 Hz, 2H, Ph), 6.97 (br s, 2H, imidazolyl), 4.49 (s, 2H, CH_2). MS (ESI): calcd for $C_{13}H_{12}N_6S$ $[M + H]^+$, 285.08; found, 285.00. HPLC: 6.906 min; purity, 98%.

2-Benzoyl-3,3-bis(methylthio)acrylonitrile (16).[45] A solution of benzoylacetonitrile **15** (1.189 g, 8.2 mmol, 1.0 equiv) in 16 mL of dry DMSO was added dropwise to a stirred suspension of 60% NaH dispersion in mineral oil (0.656 g, 16.4 mmol, 2.0 equiv) in 16 mL of dry DMSO under the N_2 condition at room temperature. Carbon disulfide (0.49 mL, 8.2 mmol, 1.0 equiv) was added dropwise under external water bath cooling, and the mixture was stirred for 2 h. Iodomethane (1.0 mL, 16.4 mmol, 2.0 equiv) was then added to the mixture dropwise under external water bath cooling, and the reaction was stirred overnight. The reaction progress was monitored by TLC. After the completion of the reaction, the mixture was poured into 600 mL of ice-cold water, and the precipitate formed was filtered and dried *in vacuo* to provide **16** in good yield (1.677 g, 6.72 mmol, 82%). ^{1}H NMR (400 MHz, DMSO) δ 7.85 (d, J = 7.2 Hz, 2H, Ph), 7.67 (t, J = 7.6 Hz, 1H, Ph), 7.55 (t, J = 7.6 Hz, 2H, Ph), 2.80 (s, 3H, CH_3), 2.53 (s, 3H, CH_3).

2-Amino-4-(methylthio)-6-phenylpyrimidine-5-carbonitrile (17).[46] A solution of **16** (0.168 g, 6.73 mmol, 1.0 equiv), guanidine hydrochloride (0.643 g, 6.73 mmol, 1.0 equiv), and triethylamine (2.34 mL, 16.8 mmol, 2.5 equiv) in 21 mL of DMF was heated at reflux for 6 h. The reaction progress was monitored by TLC. After the completion of the reaction, the mixture was cooled down to room temperature and 32 mL of water was added to cause precipitation. The precipitate was collected by filtration and washed with water and methanol to give compound **17** as a pale yellow solid (680 mg, 2.83 mmol, 42%). ^{1}H NMR (400 MHz, DMSO) δ 7.88 (br s, 1H, 0.5 NH_2), 7.81 (br s, 1H, 0.5 NH_2) 7.80−7.78 (m, 2H, Ph), 7.57−7.51 (m, 3H, Ph), 2.58 (s, 3H, CH_3).

2-Amino-4-(methylsulfinyl)-6-phenylpyrimidine-5-carbonitrile (18).[46] Intermediate **17** (0.706 g, 2.92 mmol, 1.0 equiv) was dissolved in 10 mL of CH_2Cl_2 at room temperature, and mCPBA (0.808 g, 4.68 mmol, 1.6 equiv) was added to the mixture. The mixture was stirred at room temperature for 3.5 h and monitored by TLC. The precipitate formed in the reaction was filtered, washed by CH_2Cl_2, and dried under reduced pressure to obtain **18** (495 mg, 1.93 mmol, 66%). ^{1}H NMR (400 MHz, DMSO) δ 8.39 (br s, 1H, 0.5 NH_2), 8.32 (br s, 1H, 0.5 NH_2), 7.84 (d, J = 7.2 Hz, 2H, Ph), 7.64−7.54 (m, 3H, Ph), 2.93 (s, 3H, CH_3).

2-Amino-4-sulfanyl-6-phenylpirimidine-5-carbonitrile (19).[47] To a stirred suspension of **18** (0.495 g, 1.92 mmol, 1.0 equiv) in 17 mL of DMF was added potassium thioacetate (0.376 g, 3.84 mmol, 2.0 equiv), and the mixture was stirred at room temperature for 19 h. The reaction progress was monitored by TLC. After the completion of the reaction, the mixture was cooled down in an external ice water bath, and 17 mL of 2 M aqueous NaOH was added to the cold solution. The mixture was stirred for another 1.5 h and diluted with 17 mL of H_2O, followed by pH adjustment to 5−6 with the addition of 1 M HCl (±50 mL). The mixture was diluted with 70 mL of H_2O and stirred for 1 h at room temperature. The precipitate formed in the mixture was collected by filtration, washed with H_2O (25 mL × 3), and dried under reduced pressure to give **19** in good yield (232 mg, 1.02 mmol, 53%). ^{1}H NMR (400 MHz, DMSO) δ 12.91 (br s, 1H, SH), 8.67 (br s, 1H, 0.5 NH_2), 7.78 (d, J = 7.6 Hz, 2H, Ph), 7.61−7.48 (m, 3H, Ph), 6.95 (br s, 1H, 0.5 NH_2).

https://doi.org/10.1021/acs.jmedchem.0c01856
J. Med. Chem. 2021, 64, 3827−3842

*4-((1H-Imidazol-2-yl)methylthio)-2-amino-6-phenylpyrimidine-5-carbonitrile (**3**).* Similar procedure as synthesis of **1** using **19** (0.187 g, 0.82 mmol, 1.0 equiv) as a starting material to afford a light yellow solid (116 mg; 0.38 mmol; yield, 46%). Mp 224 °C. ^{1}H NMR (400 MHz, DMSO) δ 11.86 (br s, 1H, NH), 7.97 (m, 2H, NH_2), 7.79 (d, J = 6.8 Hz, 2H, Ph), 7.60−7.50 (m, 3H, Ph), 7.08 (br s, 1H, imidazolyl), 6.85 (br s, 1H, imidazolyl), 4.53 (s, 2H, CH_2). MS (ESI): calcd for $C_{15}H_{12}N_6S$ $[M + H]^+$, 309.08; found, 309.00. HPLC: 4.377 min; purity: 99%.

*2-(1-Phenylethylidene)malononitrile (**21**).*[25] The synthesis of this compound was adapted from the conditions previously described by Longstreet *et al.*[25] A mixture of acetophenone **20** (2.80 mL, 24 mmol, 1.0 equiv), malononitrile (1.586 g, 24.00 mmol, 1 equiv), and ammonium acetate (0.370 g, 4.80 mmol, 0.2 equiv) in toluene (20 mL) was heated at reflux under Dean−Stark conditions for 5 h. The reaction progress was monitored by TLC. After the completion of the reaction, the mixture was cooled down to room temperature. The reaction was diluted with EtOAc (50 mL), washed with saturated $NaHCO_3$ solution (50 mL × 3) followed by water (50 mL), dried over $MgSO_4$, and concentrated *in vacuo* to obtain a brown oil, which solidified at room temperature after 30 min. Purification was performed by column chromatography (CH_2Cl_2) to obtain **21** as a white solid (2.82 g, 16.8 mmol, 70%). ^{1}H NMR (400 MHz, $CDCl_3$) δ 7.58−7.26 (m, 5H, Ph), 2.64 (s, 3H, CH_3). HNMR is consistent with the reported literature data.

*2-Amino-6-(methylthio)-4-phenylnicotinonitrile (**22**).*[48] A mixture of **21** (2.5 g, 14.86 mmol, 1.0 equiv), dimethyl cyanocarbonimidodithioate (3.69 g, 25.3 mmol, 1.7 equiv), and potassium carbonate (2.465 g, 17.84 mmol, 1.2 equiv) in DMF (30 mL) was stirred at room temperature for 6 h. After the completion of the reaction, piperidine (2.4 mL, 23.78 mmol, 1.6 equiv) was added and the mixture was stirred at 80 °C overnight. The reaction progress was monitored by TLC. The mixture was then concentrated *in vacuo*, diluted with water, and extracted three times with CH_2Cl_2. The organic layer was dried over $MgSO_4$ and concentrated *in vacuo*. The brown oil obtained was purified by column chromatography (CH_2Cl_2), yielding **22** as a yellow solid (2.21 g, 9.21 mmol, 62%). ^{1}H NMR (400 MHz, $CDCl_3$) δ 7.56−7.52 (m, 2H, Ph), 7.49−7.47 (m, 3H, Ph), 6.64 (s, 1H, pyridinyl), 5.27 (br s, 2H, NH_2), 2.54 (s, 3H, CH_3).

*2-Amino-6-(methylsulfonyl)-4-phenylnicotinonitrile (**23**).* A mixture of **22** (1 g, 4.14 mmol, 1 equiv) and mCPBA (1.114 g, 4.97 mmol, 1 equiv) in 120 mL of CH_2Cl_2 was stirred at room temperature for 5 min. The mixture was then washed twice with $NaHCO_3$ solution followed by water, dried over $MgSO_4$, and concentrated *in vacuo* to yield a mixture of sulfoxide and sulfone product. Without further separation, it was then reacted with 77 wt % mCPBA (0.674 g, 3.90 mmol, 0.94 equiv) in CH_2Cl_2 (70 mL) and stirred at room temperature for another 5 min. The mixture was washed twice with $NaHCO_3$ solution followed by water, dried over $MgSO_4$, and concentrated *in vacuo*. Purification was performed by column chromatography (2% MeOH in CH_2Cl_2), yielding **23** as a yellow solid (0.631 g, 2.31 mmol, 56%). ^{1}H NMR (400 MHz, DMSO) δ 7.68−7.65 (m, 4H, NH_2 + Ph), 7.59−7.57 (m, 3H, Ph), 7.17 (s, 1H, pyridinyl), 3.27 (s, 3H, CH_3).

*2-Amino-6-sulfanyl-4-phenylnicotinonitrile (**24**).* A mixture of **23** (0.631 g, 2.31 mmol, 1 equiv) and potassium ethanethioate (0.527 g, 4.62 mmol, 2 equiv) in DMF (8 mL) was stirred at 80 °C for 4 h. After the completion of the reaction as shown by TLC, 2 M NaOH solution was added and the mixture was stirred at room temperature for another 2 h. The mixture was then diluted with water (80 mL) and 1 M HCl solution was added to adjust pH to 1. The precipitate formed was filtered and dried *in vacuo* to obtain a brown crude solid. Purification was performed by column chromatography (3% MeOH in CH_2Cl_2) to obtain the product as a yellow solid (0.321 g, 1.41 mmol, 61%). ^{1}H NMR (400 MHz, DMSO) δ 12.58 (s, 1H, SH), 7.58−7.48 (m, 6H), 7.31 (br s, 2H, NH_2), 6.47 (s, 1H). MS (ESI): calcd for $C_{12}H_9N_3S$ $[M + H]^+$, 228.05; found, 228.13.

*6-(((1H-Imidazol-2-yl)methyl)thio)-2-amino-4-phenylnicotinonitrile (**4**).* A mixture of **24** (0.12 g, 0.66 mmol, 1 equiv), 7 (0.16 g, 0.66 mmol, 1 equiv), and $NaHCO_3$ (0.166 g, 1.98 mmol, 2 equiv) in DMF (3 mL) was stirred at 50 °C for 4 h. After the completion of the reaction as shown by TLC, the mixture was concentrated *in vacuo* and dissolved in EtOAc followed by washing three times with water and brine. The organic phase was dried over $MgSO_4$, concentrated *in vacuo* to give a crude yellow oil, and purified by dry-loaded column chromatography (5% MeOH in CH_2Cl_2) as a column chromatography eluent. Compound **4** was obtained as a white solid (0.115 g; 0.376 mmol; yield, 57%). Mp 220 °C. ^{1}H NMR (400 MHz, DMSO) δ 11.86 (br s, 1H, NH), 7.587.53 (m, 2H, Ph), 7.52−7.49 (m, 3H, Ph), 7.17 (br s, 2H, NH_2), 7.05 (br s, 1H, imidazolyl), 6.82 (br s, 1H, imidazolyl), 6.68 (s, 1H, pyridinyl), 4.39 (s, 2H, CH_2). MS (ESI): calcd for $C_{16}H_{13}N_5S$ $[M + H]^+$, 308.09; found, 308.05. HPLC: 6.33 min; purity: 99%.

*2,6-Dichloro-4-phenylpyridine (**26**).*[49] A stirred suspension of 2,6-dichloro-4-iodopyridine **25** (1 g, 3.65 mmol, 1.0 equiv), Na_2CO_3 (1.16 g, 10.95 mmol, 3.0 equiv), phenylboronic acid pinacol ester (0.745 g, 3.65 mmol, 1.0 equiv), and $Pd(PPh_3)_2Cl_2$ (0.128 g, 0.183 mmol, 0.05 equiv) in a mixture of acetonitrile (12 mL) and H_2O (8 mL) under a N_2 atmosphere was heated at 70 °C for 16 h. The reaction progress was monitored by TLC (2% EtOAc in PET) and HPLC. The mixture was diluted with EtOAc (50 mL) and washed with brine (30 mL × 3). The organic layer was dried over $MgSO_4$ and evaporated under reduced pressure. The resulting brown oil was purified by column chromatography (2% EtOAc in PET) to afford a white solid (750 mg, 3.36 mmol, 92%). ^{1}H NMR (400 MHz, $CDCl_3$) δ 7.61−7.57 (m, 2H, Ph), 7.53−7.48 (m, 3H, Ph), 7.47 (s, 2H, pyridinyl). HNMR in accordance with the literature.

*2-(tert-Butylthio)-6-chloro-4-phenylpyridine (**27**).* A suspension of 2,6-dichloro-4-phenylpyridine **26** (0.2 g, 0.89 mmol, 1.0 equiv), Cs_2CO_3 (0.58 g, 1.78 mmol, 2.0 equiv), and 2-methylpropane-2-thiol (0.084 g, 0.93 mmol, 1.04 equiv) in DMF was heated at 80 °C overnight. The reaction progress was monitored by TLC (10% EtOAc in PET) and HPLC. The mixture was diluted with EtOAc (50 mL) and washed with brine (30 mL × 5). The organic phase was dried on $MgSO_4$ and evaporated to afford a pale yellow oil (249 mg, 0.89 mmol, quantitative yield). ^{1}H NMR (400 MHz, $CDCl_3$) δ 7.69−7.54 (m, 2H, Ph), 7.50−7.43 (m, 3H, Ph), 7.37 (d, J = 1.2 Hz, 1H, pyridinyl), 7.26 (d, J = 1.2 Hz, 1H, pyridinyl) 1.59 (s, 9H, *t*-butyl). MS (ESI): calcd for $C_{15}H_{16}ClNS$ $[M + H]^+$, 278.07; found, 277.90.

*tert-Butyl-(6-(tert-butylthio)-4-phenylpyridin-2-yl)-carbamate (**28**).* A suspension of 2-(*tert*-butylthio)-6-chloro-4-phenylpyridine **27** (0.23 g, 0.83 mmol, 1.0 equiv), Cs_2CO_3 (0.54 g, 1.66 mmol, 2.0 equiv), Xantphos (0,144 g, 0.25 mmol, 0.3 equiv), $Pd(OAc)_2$ (0.028 g, 0.124 mmol, 0.15 equiv), and *t*-butyl carbamate (0.097 g, 0.83 mmol, 1.0 equiv) in dry 1,4-dioxane (2.8 mL) under a N_2 atmosphere was heated at 110 °C overnight. The reaction progress was monitored by TLC (2% EtOAc in PET) and HPLC. The mixture was treated with warm acetone (25 mL) and filtered. The organic layer was evaporated and purified by column chromatography (20% EtOAc in PET) to afford **28** as a yellow solid (80 mg, 0.22 mmol, 27%). ^{1}H NMR (400 MHz, DMSO) δ 9.96 (s, 1H, NH), 7.84 (d, J = 1.6 Hz, 1H), 7.67 (d, J = 6.8 Hz, 2H, Ph), 7.54−7.44 (m, 3H, Ph), 7.15 (d, J = 1.6 Hz, 1H), 1.53 (s, 9H), 1.50 (s, 9H). MS (ESI): calcd for $C_{20}H_{26}N_2O_2S$ $[M + H]^+$, 359.17; found, 358.9.

*6-(tert-Butylthio)-4-phenylpyridin-2-amine (**29**).* To a solution of *tert*-butyl (6-(*tert*-butylthio)-4-phenylpyridin-2-yl)-carbamate **28** (0.25 g, 0.697 mmol, 1.0 equiv) in CH_2Cl_2 (5 mL) was added TFA (0.266 mL, 3.48 mmol, 5.0 equiv). The mixture was refluxed overnight. The reaction progress was monitored by TLC (6% MeOH in CH_2Cl_2) and HPLC. The mixture was diluted with EtOAc (50 mL) and washed with H_2O (25 mL × 4). The organic phase was dried on $MgSO_4$ and evaporated to afford a brown oil. The crude compound was purified by liquid chromatography (50% EtOAc in PET) to give **29** as a pale yellow oil (135 mg, 0.523 mmol, 75%). ^{1}H NMR (400 MHz, DMSO) δ 7.66 (dd, J = 6.8, 2.0 Hz, 2H, Ph), 7.54−7.47 (m, 3H, Ph), 6.96 (s br, 1H, 0.5 NH_2), 6.76 (s br, 1H, 0.5 NH_2), 1.46 (s, 9H, *t*-butyl). MS (ESI): calcd for $C_{15}H_{18}N_2S$ $[M + H]^+$, 259.12; found, 259.0 $[M + H]^+$.

https://doi.org/10.1021/acs.jmedchem.0c01856
J. Med. Chem. 2021, 64, 3827−3842

*6-Amino-4-phenylpyridine-2-thiol (**30**).* A stirred solution of 6-(*tert*-butylthio)-4-phenylpyridin-2-amine **29** (0.445 g, 1.722 mmol) in 37% HCl (15 mL) was heated at 100 °C for 10 h. The reaction progress was monitored by HPLC. The mixture was carefully treated with $NaHCO_3$ saturated solution to pH = 7 and extracted with EtOAc (40 mL × 5). The organic phase was dried over $MgSO_4$ and evaporated to afford an orange solid (135 mg, mixture of the desired compound and the corresponding dimer). The compound was used for the next reaction without further purification. ^{1}H NMR (400 MHz, DMSO) δ 12.25 (s br, 1H, SH), 7.59−7.55 (m, 2H, Ph), 7.49−7.43 (m, 3H, Ph), 6.85 (s br, 1H, 0.5 NH_2), 6.40 (s br, 1H, 0.5 NH_2). MS (ESI): calcd for $C_{11}H_{10}N_2S$ $[M + H]^+$, 203.06; found, 203.1.

*6-(((1H-Imidazol-2-yl)methyl)thio)-4-phenylpyridin-2-amine (**5**).* To a suspension of 6-amino-4-phenylpyridine-2-thiol **30** (0.145 g, 0.716 mmol, 1.0 equiv) and $NaHCO_3$ (0.061 g, 0.57 mmol, 0.8 equiv) in dry DMF (2 mL) was added **7** (0.225 g, 0.931 mmol, 1.3 equiv). The mixture was stirred at room temperature for 23 h. The reaction progress was monitored by HPLC. DMF was evaporated under reduced pressure (water bath at 70 °C). The resulting residue was treated with H_2O (20 mL) and extracted with EtOAc (30 mL × 4). The organic phase was dried over $MgSO_4$ and evaporated to afford an orange oil. The compound was purified by liquid chromatography (10% MeOH in CH_2Cl_2) to obtain pure **5** as a pale red solid (67 mg; 0.24 mmol; yield, 33%). Mp 109 °C. ^{1}H NMR (400 MHz, MeOD) δ 7.55−7.50 (m, 2H, Ph), 7.46−7.32 (m, 3H, Ph), 6.94 (s, 2H, pyridinyl), 6.70 (d, J = 1.2 Hz, 1H, imidazolyl), 6.50 (d, J = 1.2 Hz, 1H, imidazolyl), 4.39 (s, 2H, CH_2). MS (ESI): calcd for $C_{15}H_{14}N_4S$ $[M + H]^+$, 283.09; found, 283.00. HPLC: 3.722 min; purity: 97%.

*2,6-Dihydroxy-4-phenylnicotinonitrile (**32**).*[30] A suspension of commercially available ethylbenzoyl acetate **31** (3 g, 15.6 mmol, 1.0 equiv), 2-cyanoacetamide (1.31 g, 15.6 mmol, 1.0 equiv), and KOH (0.96 g, 15.6 mmol, 1.0 equiv) in EtOH (20 mL) was refluxed for 24 h. The reaction progress was monitored by HPLC and TLC (20% MeOH in CH_2Cl_2). After the completion of the reaction, the mixture was cooled down to 0 °C. The suspended solid was collected by filtration and subsequently dissolved in warm water (60 mL). The alkaline solution was carefully treated with 37% HCl solution to adjust the pH to 1. The precipitate was collected by filtration and dried to give **32** in good yield (1.3 g, 5.3 mmol, 34%). ^{1}H NMR (400 MHz, DMSO) δ 7.52 (s, 5H, Ph), 5.80 (s, 1H, pyridinyl). MS (ESI): calcd for $C_{12}H_8N_2O2$ $[M + H]^+$, 213.06; found, 213.1. HNMR is consistent with the reported literature data.

*2,6-Dichloro-4-phenylnicotinonitrile (**33**).* A suspension of 2,6-dihydroxy-4-phenylnicotinonitrile **32** (1.2 g, 5.657 mmol, 1.0 equiv) in $POCl_3$ (5.3 mL, 56.6 mmol, 10.0 equiv) was heated at 180 °C in an autoclave for 16 h. The reaction progress was monitored by HPLC. The mixture was cooled down to 0 °C and treated with crushed ice. The suspended solid was collected by filtration, rinsed with petroleum ether (30 mL), and dried under reduced pressure to afford **33** as a gray solid (0.990 g, 3.96 mmol, 70%). ^{1}H NMR (400 MHz, $CDCl_3$) δ 7.63−7.60 (m, 5H, Ph), 7.45 (s, 1H, pyridinyl). HNMR is consistent with the reported literature data.

*tert-Butyl-(6-chloro-5-cyano-4-phenylpyridin-2-yl)-carbamate (**34**).* To a suspension of 2,6-dichloro-4-phenylnicotinonitrile **33** (0.2 g, 0.806 mmol, 1.0 equiv), *t*-butyl carbamate (0.095 g, 0.806 mmol, 1.0 equiv), Cs_2CO_3 (0.54 g, 1.66 mmol, 2.06 equiv), and Xantphos (0.139 g, 0.242 mmol, 0.3 equiv) in dry 1,4-dioxane (2.7 mL) under a N_2 atmosphere was added $Pd(OAc)_2$ (0.027 g, 0.121 mmol, 0.15 equiv). The mixture was heated at 40 °C for 23 h. The reaction progress was monitored by TLC (2% EtOAc in PET) and HPLC. The mixture was then treated with warm acetone (25 mL) and filtered. The organic layer was evaporated to afford a pale brown solid (90 mg, 0.26 mmol, 33%). The product was used for the next reaction without further purification. ^{1}H NMR (300 MHz, $CDCl_3$) δ 8.07 (s, 1H, pyridinyl), 7.64−7.58 (m, 2H, Ph), 7.55−7.47 (m, 4H, Ph + NH), 1.53 (s, 9H, *t*-butyl). MS (ESI): calcd for $C_{17}H_{16}ClN_3O_2$ $[M + H]^+$, 330.09; found, 329.92.

*tert-Butyl (6-(tert-butylthio)-5-cyano-4-phenylpyridin-2-yl)-carbamate (**35**).* A suspension of *tert*-butyl (6-chloro-5-cyano-4-phenylpyridin-2-yl)-carbamate **34** (0.09 g, 0.273 mmol, 1.0 equiv), 2-methyl-propanethiol (0.03 mL, 0.273 mmol, 1.0 equiv), and Cs_2CO_3 (0.178 g, 0.56 mmol, 2 equiv) in DMF (2 mL) was heated at 90 °C for 20 h. The reaction progress was monitored by HPLC. The mixture was cooled down to room temperature, diluted with EtOAc (50 mL), and washed with brine (25 mL × 5). The organic layer was dried on $MgSO_4$ and evaporated to afford an orange oil (93 mg, 0.211 mmol, 89%). The compound was used for the next reaction without further purification. ^{1}H NMR (400 MHz, $CDCl_3$) δ 7.81 (s, 1H, pyridinyl), 7.59−7.55 (m, 2H, Ph), 7.48−7.44 (m, 3H, Ph), 7.32 (s br, 1H, NH), 1.65 (s, 9H, *t*-butyl), 1.54 (s, 9H, *t*-butyl). MS (ESI): calcd for $C_{21}H_{25}N_3O_2S$ $[M + H]^+$, 384.17; found, 284.00.

*6-Amino-2-sulfanyl-4-phenylnicotinonitrile (**36**).* A suspension of **35** (0.7 g, 1.825 mmol) in 37% HCl (7 mL) was heated at 100 °C for 2 h. The reaction progress was monitored by HPLC. The mixture was cooled down to room temperature and diluted with $NaHCO_3$ saturated solution (7 mL). The resulting suspension was treated carefully with solid $NaHCO_3$ to pH 7 and extracted with EtOAc (30 mL × 5). The organic layer was dried over $MgSO_4$ and evaporated to afford an orange solid, which was purified by column chromatography (40% EtOAc in PET and 10% MeOH in CH_2Cl_2). Intermediate **36** was obtained as a pale yellow solid (156 mg, 0.675 mmol, 37%). ^{1}H NMR (400 MHz, MeOD) δ 7.56−7.51 (m, 2H, Ph), 7.51−7.47 (m, 3H, Ph), 6.05 (s, 1H, pyridinyl). MS (ESI): calcd for $C_{12}H_9N_3S$ $[M + H]^+$, 228.05; found, 228.08.

*2-(((1H-Imidazol-2-yl)methyl)thio)-6-amino-4-phenylnicotinonitrile (**6**).* A suspension of **36** (0.096 g, 0.422 mmol, 1.0 equiv), $NaHCO_3$ (0.020 g, 0.422 mmol, 1.0 equiv), and **7** in dry DMF (2.5 mL) was stirred at room temperature for 4 h. The reaction progress was monitored by TLC (10% MeOH in CH_2Cl_2). DMF was evaporated under reduced pressure (water bath at 70 °C). The resulting residue was treated with water (10 mL) and extracted with EtOAc (30 mL × 5). The organic layer was dried over $MgSO_4$ and evaporated to afford a pale brown oil. The final compound **6** was obtained after purification by column chromatography (PET/EtOAc/MeOH, 1:7.8:1.2) and recrystallized using diethyl ether and MeOH to yield **6** as a pale yellow solid (10 mg; 0.032 mmol; yield, 8%). Mp 222 °C. ^{1}H NMR (400 MHz, MeOD) δ 7.53−7.45 (m, 5H, Ph), 6.97 (s, 2H, imidazolyl), 6.28 (s, 1H, pyridinyl), 4.53 (s, 2H, CH_2). MS (ESI): calcd for $C_{16}H_{13}N_5S$ $[M + H]^+$, 308.09; found, 308.00. HPLC: 7.490 min; purity: 99%.

Pharmacology. *Cell Lines and Chemicals.* Chinese hamster ovary (CHO) cells stably expressing the human adenosine A_1 receptor ($CHOhA_1R$) were kindly provided by Prof. S. J. Hill (University of Nottingham, U.K.), human embryonic kidney 293 cells stably expressing the human adenosine A_{2A} receptor ($HEK_{293}hA_{2A}R$) were kindly provided by Dr. J. Wang (Biogen/IDEC, Cambridge, MA), CHO-spap cells stably expressing the wild-type (WT) hA_{2B} receptor (CHO-spap-$hA_{2B}R$) were kindly provided by S. J. Dowell (GlaxoSmithKline, U.K.), and CHO cells stably expressing the human adenosine A_3 receptor ($CHOhA_3R$) were a gift from Dr. K.-N. Klotz (University of Würzburg, Germany). [^{3}H]1,3-Dipropyl-8-cyclopentylxanthine ([^{3}H]DPCPX; specific activity, 120 Ci/mmol) was purchased from ARC, Inc. (St. Louis, USA), [^{3}H]4-(2-[7-amino-2-(furan-2-yl)-[1,2,4]triazolo[1,5-*a*][1,3,5]triazin-5-ylamino)ethyl) phenol ([^{3}H]-ZM241385; specific activity, 50 Ci/mmol) was purchased from ARC, Inc. (St. Louis, USA), [^{3}H]8-(4-(4-(4-chlorophenyl)-piperazide-1-sulfonyl)phenyl)-1-propylxanthine ([^{3}H]PSB-603; specific activity, 79 Ci/mmol) was purchased from Quotient Bioresearch (Waltham, MA), and [^{3}H]8-ethyl-4-methyl-2-phenyl-(8*R*)-4,5,7,8-tetrahydro-1*H*-imidazo[2,1-*i*]-purin-5-one ([^{3}H]PSB-11; specific activity, 56 Ci/mmol) was obtained with the kind help of Prof. C. E. Müller (University of Bonn, Germany). 5′-*N*-Ethylcarboxamidoadenosine (NECA), N^6-cyclopentyladenosine (CPA), and adenosine deaminase (ADA) were purchased from Sigma-Aldrich (Steinheim, Germany). Unlabeled 4-(2-[7-amino-2-(furan-2-yl)-[1,2,4]triazolo-[1,5-*a*][1,3,5]triazin-5-ylamino)ethyl) phenol (ZM241385) was a kind gift from Dr. S. M. Poucher (Astra Zeneca, Manchester, U.K.). 3-[4-[2-[[6-Amino-9-[(2*R*,3*R*,4*S*,5*S*)-5-(ethylcarbamoyl)-3,4-dihydroxy-oxolan-2-yl]purin-2-yl]amino]ethyl]phenyl] propanoic acid (CGS21680) was purchased from Ascent Scientific (Bristol, U.K.).

https://doi.org/10.1021/acs.jmedchem.0c01856
J. Med. Chem. 2021, 64, 3827−3842

Bicinchoninic acid (BCA) protein assay reagents were obtained from Pierce Chemical Company (Rockford, IL, USA). All other chemicals were of analytical grade and were obtained from standard commercial sources.

Cell Culture and Membrane Preparation. $CHOhA_1R$ and $CHOhA_3R$ cells were grown in Dulbecco's modified Eagle's medium (DMEM) and Ham's F12 medium (1:1) supplemented with 10% (v/v) newborn calf serum, 50 $\mu g \cdot mL^{-1}$ streptomycin, 50 $IU \cdot mL^{-1}$ penicillin, and 200 $\mu g \cdot mL^{-1}$ G418 at 37 °C and 5% CO_2. $CHOhA_1R$ cells were subcultured twice a week at a ratio of 1:20 on 10 cm Ø plates and 15 cm Ø plates. $CHOhA_3$ cells were subcultured twice a week at a ratio of 1:8 on 10 cm Ø plates and 15 cm Ø plates. $HEK_{293}hA_{2A}R$ cells were grown in a culture medium consisting of Dulbecco's modified Eagle's medium (DMEM) supplemented with 10% newborn calf serum, 50 $\mu g \cdot mL^{-1}$ streptomycin, 50 $IU \cdot mL^{-1}$ penicillin, and 500 $\mu g \cdot mL^{-1}$ G418 at 37 °C and 7% CO_2. Cells were subcultured twice a week at a ratio of 1:8 on 10 cm Ø plates and 15 cm Ø plates. CHO-spap-$hA_{2B}R$ cells were grown in Dulbecco's modified Eagle's medium (DMEM) and Ham's F12 medium (1:1) supplemented with 10% (v/v) newborn calf serum, 100 $\mu g \cdot mL^{-1}$ streptomycin, 100 $IU \cdot mL^{-1}$ penicillin, 1 $mg \cdot mL^{-1}$ G418, and 0.4 $mg \cdot mL^{-1}$ hygromycin at 37 °C and 5% CO_2. Cells were subcultured at a ratio of 1:20 twice weekly.

All cells were grown to 80−90% confluency and detached from plates by scraping them into 5 mL of PBS. Detached cells were collected and centrifuged at 200*g* for 5 min. Pellets derived from 100 15 cm Ø plates were pooled and resuspended in 70 mL of ice-cold 50 mM Tris−HCl buffer (pH 7.4). A Heidolph Diax 900 homogenizer was used to homogenize the cell suspension. Membranes and the cytosolic fraction were separated by centrifugation at 100,000*g* in a Beckman Optima LE-80K ultracentrifuge (Beckman Coulter, Fullerton, CA) at 4 °C for 20 min. The pellet was resuspended in 35 mL of Tris−HCl buffer, and the homogenization and centrifugation steps were repeated. Tris−HCl buffer (25 mL) was used to resuspend the pellet, and ADA was added (0.8 U/mL) to break down endogenous adenosine. Membranes were stored in 250 and 500 μL aliquots at −80 °C. Total protein concentrations were measured using the BCA method.[50]

Radioligand Binding Studies. Membrane aliquots containing 5 μg ($CHOhA_1R$) or 30 μg ($HEK_{293}hA_{2A}R$) of total protein were incubated in a total volume of 100 μL assay buffer (50 mM Tris−HCl, pH 7.4) at 25 °C for 1 h. Membrane aliquots containing 30 μg (CHO-spap-$hA_{2B}R$) of total protein were incubated in a total volume of 100 μL assay buffer (0.1% CHAPS in 50 mM Tris−HCl, pH 7.4) at 25 °C for 2 h, or those containing 15 μg ($CHOhA_3R$) of total protein were incubated in a total volume of 100 μL assay buffer (50 mM Tris−HCl, pH 8.0, supplemented with 10 mM $MgCl_2$, 1 mM EDTA, and 0.01% (w/v) CHAPS) at 25 °C for 2 h. Radioligand displacement experiments were performed using six concentrations of the competing ligand in the presence of 1.6 nM [^{3}H]DPCPX for $CHOhA_1R$, 5.5 nM [^{3}H]ZM241385 for $HEK_{293}hA_{2A}R$, 1.5 nM [^{3}H]PSB-603 for CHO-spap-$hA_{2B}R$, and 10 nM [^{3}H]PSB-11 for $CHOhA_3R$. At these concentrations, the total radioligand binding did not exceed 10% of that added to prevent ligand depletion. Nonspecific binding was determined in the presence of 100 μM CPA for $CHOhA_1R$, 100 μM NECA for $HEK_{293}hA_{2A}R$ and $CHOhA_3R$, and 10 μM ZM241385 for CHO-spap-$hA_{2B}R$. Incubations were terminated by rapid vacuum filtration to separate the bound and free radioligands through prewetted 96-well GF/B filter plates using a PerkinElmer Filtermate-harvester (PerkinElmer, Groningen, The Netherlands). Filters were subsequently washed 12 times with ice-cold wash buffer: 50 mM Tris−HCl (pH 7.4) for $CHOhA_1R$ and $HEK_{293}hA_{2A}R$, 0.1% BSA in 50 mM Tris−HCl (pH 7.4) for CHO-spap-$hA_{2B}R$, and 50 mM Tris−HCl supplemented with 10 mM $MgCl_2$ and 1 mM EDTA (pH 8.0) for $CHOhA_3R$. The plates were dried at 55 °C after which MicroScint-20 cocktail was added (PerkinElmer, Groningen, The Netherlands). After 3 h, the filter-bound radioactivity was determined by scintillation spectrometry using a 2450 MicroBeta Microplate Counter (PerkinElmer, Groningen, The Netherlands).

Label-Free Impedance-Based Assay. Label-free whole-cell assays were performed on the xCELLigence real-time cell analyzer (RTCA) system.[51,52] In this system, the cells are adhered to arrayed gold electrodes embedded at the bottom of microelectronic E-plate 96 (Bioké, Leiden, NL), which is compatible with the xCELLigence RTCA system (ACEA Bioscience, San Diego, CA, USA). Upon activation of GPCR-mediated signaling, the cell morphology changes and therefore affects the local ionic environment at the cell−electrode interface. This leads to an increased electronic readout of cell-sensor impedance (Z), which is displayed in real time as the cell index (CI). Specifically, the CI value at each time point is defined as $(Z_i - Z_0)\Omega/15\Omega$, where Z_i is the impedance at each individual time point, and Z_0 is the impedance derived from the electrode/solution interface in the absence of cells prior to the start of the experiment. $HEK293hA_{2A}R$ cells were cultured as a monolayer on 10 cm Ø culture plates to 80−90% confluency and subsequently harvested and centrifuged two times at 1000 rpm for 5 min. Initially, 45 μL of culture media was added to wells in E-plates 96 to obtain background readings (Z_0) followed by the addition of 50 μL of cell suspension containing 20,000 cells/well. The E-plate containing the cells was left at room temperature for 30 min before being placed on the recording device station in the incubator at 37 °C in 7% CO_2. Afterward, cell attachment, spreading, and proliferation were continuously monitored every 15 min. The cells were cultured until the end of log phase (~18−20 h) to obtain an optimal assay window. Prior to agonist application (either the reference compound CGS21680, **8**, or newly synthesized compounds), the interval between two measurements was adjusted to 15 s. Subsequently, 5 μL of compound solution (final concentration of 0.1% DMSO) or vehicle control (0.1% DMSO) was added to each well, after which the CI was recorded for 60 min.

Molecular Modeling. All preparations and simulations were performed using Schrödinger Suite.[53] The crystal structure of $hA_{2A}AR$ in complex with compound **8** was obtained in-house (*vide supra*) and used for the *in silico* experiment. All thermostabilizing mutations were reverted to wild-type $hA_{2A}AR$, the bRIL fusion protein was removed from the crystal structure, and the third intracellular loop (ICL3) was filled in using Prime.[3,33,54] Missing water molecules in the binding pocket of the crystal structure were added from 4EIY.[3] The protein was prepared by the "Protein Preparation Wizard" at default settings. The compounds (**1** and **3**) were built and prepared using LigPrep.[55] Induced-fit docking[34] was performed flexibly with the crystal ligand **8** as the center of workspace in the standard protocol and OPLS3 as the force field. Figures were rendered using PyMol.[56]

Data Analysis. All experimental data were analyzed using the nonlinear regression curve fitting program GraphPad Prism 7.0 (GraphPad Software Inc., San Diego, CA). IC_{50} values obtained from competition displacement binding data were converted into K_i values using the Cheng−Prusoff equation.[57] The K_D value of [^{3}H]DPCPX (1.6 nM) at $CHOhA_1R$ membranes was taken from Kourounakis *et al.*[58] The K_D value (1.0 nM) of [^{3}H]ZM241385 at $hA_{2A}R$ membranes, the K_D value (1.71 nM) of [^{3}H]PSB-603 at CHO-spap-$hA_{2B}R$ membranes, and the K_D value (17.3 nM) of [^{3}H]PSB-11 at $CHOhA_3R$ membranes were taken from in-house determinations. Efficacy data from xCELLigence were obtained using RTCA software 1.2 (Roche, Germany) by normalizing CI traces to define peak responses within 60 min after compound addition. Peak values were used further for the determination of concentration−effect curves, yielding EC_{50} (concentration causing a half-maximum effect) and E_{max} (maximum effect relative to CGS21680) values.

■ ASSOCIATED CONTENT

Supporting Information

The Supporting Information is available free of charge at https://pubs.acs.org/doi/10.1021/acs.jmedchem.0c01856.

Additional figures of crystal structure and computational models (Figures S1−S3 and S5), graph of displacement curves (Figure S4), linear correlation plot (Figure S6),

https://doi.org/10.1021/acs.jmedchem.0c01856
J. Med. Chem. 2021, 64, 3827−3842

and HNMR and LCMS analyses of compounds **1**−**6** (PDF)

Molecular formula strings (CSV)

AUTHOR INFORMATION

Corresponding Author

Adriaan P. IJzerman − *Division of Drug Discovery and Safety, Leiden Academic Centre for Drug Research, Leiden University, 2333 CC Leiden, The Netherlands;* orcid.org/0000-0002-1182-2259; Phone: +31-71-5274651; Email: ijzerman@lacdr.leidenuniv.nl

Authors

Tasia Amelia − *Division of Drug Discovery and Safety, Leiden Academic Centre for Drug Research, Leiden University, 2333 CC Leiden, The Netherlands; School of Pharmacy, Bandung Institute of Technology, 40132 Bandung, Indonesia;* orcid.org/0000-0002-7414-9428

Jacobus P. D. van Veldhoven − *Division of Drug Discovery and Safety, Leiden Academic Centre for Drug Research, Leiden University, 2333 CC Leiden, The Netherlands*

Matteo Falsini − *Division of Drug Discovery and Safety, Leiden Academic Centre for Drug Research, Leiden University, 2333 CC Leiden, The Netherlands*

Rongfang Liu − *Division of Drug Discovery and Safety, Leiden Academic Centre for Drug Research, Leiden University, 2333 CC Leiden, The Netherlands*

Laura H. Heitman − *Division of Drug Discovery and Safety, Leiden Academic Centre for Drug Research, Leiden University, 2333 CC Leiden, The Netherlands;* orcid.org/0000-0003-3662-8177

Gerard J. P. van Westen − *Division of Drug Discovery and Safety, Leiden Academic Centre for Drug Research, Leiden University, 2333 CC Leiden, The Netherlands;* orcid.org/0000-0003-0717-1817

Elena Segala − *Sosei Heptares, Cambridge CB21 6DG, United Kingdom*

Grégory Verdon − *Sosei Heptares, Cambridge CB21 6DG, United Kingdom*

Robert K. Y. Cheng − *Sosei Heptares, Cambridge CB21 6DG, United Kingdom*

Robert M. Cooke − *Sosei Heptares, Cambridge CB21 6DG, United Kingdom*

Daan van der Es − *Division of Drug Discovery and Safety, Leiden Academic Centre for Drug Research, Leiden University, 2333 CC Leiden, The Netherlands*

Complete contact information is available at: https://pubs.acs.org/10.1021/acs.jmedchem.0c01856

Author Contributions

T.A., L.H.H., G.J.P.v.W., D.v.d.E., R.M.C., and A.P.IJ. were involved in the study design. E.S., G.V., and R.K.Y.C. carried out the crystal structure determination. T.A., J.P.D.v.V., M.F., and D.v.d.E. conducted synthetic chemistry experiments. R.L., L.H.H., and A.P.IJ. performed pharmacology experiments. T.A. and G.J.P.v.W. carried out the computational study. T.A., J.P.D.v.V., L.H.H., G.J.P.v.W., E.S., G.V., R.M.C., D.v.d.E., and A.P.IJ. wrote the manuscript.

Notes

The authors declare no competing financial interest.

The **8**−hA_{2A}AR complex structure coordinates and structure factors are available via the Protein Data Bank, accession code (PDB ID) 7ARO. Receptor models with compounds **1** and **3** are available as well. The authors will release the atomic coordinates and experimental data upon article publication.

ACKNOWLEDGMENTS

T.A. acknowledges financial support by the Indonesia Endowment Fund for Education (LPDP). Eelke B. Lenselink is acknowledged for his help with the computational aspects of the study.

ABBREVIATIONS USED

bRIL, thermostabilized apocytochrome b562RIL; GPCR, G protein-coupled receptor; hAR, human adenosine receptor; mCPBA, *meta*-chloroperoxybenzoic acid; RTCA, real-time cell analysis; StaR, (thermo)stabilized receptor; TFA, trifluoroacetic acid

REFERENCES

(1) Fredholm, B. B.; IJzerman, A. P.; Jacobson, K. A.; Linden, J.; Müller, C. E. International Union of Basic and Clinical Pharmacology. LXXXI. Nomenclature and classification of adenosine receptors-an update. *Pharmacol. Rev.* **2011**, *63*, 1−34.

(2) Jaakola, V.-P.; Griffith, M. T.; Hanson, M. A.; Cherezov, V.; Chien, E. Y. T.; Lane, J. R.; IJzerman, A. P.; Stevens, R. C. The 2.6 angstrom crystal structure of a human A_{2A} adenosine receptor bound to an antagonist. *Science* **2008**, *322*, 1211−1217.

(3) Liu, W.; Chun, E.; Thompson, A. A.; Chubukov, P.; Xu, F.; Katritch, V.; Han, G. W.; Roth, C. B.; Heitman, L. H.; IJzerman, A. P.; Cherezov, V.; Stevens, R. C. Structural basis for allosteric regulation of GPCRs by sodium ions. *Science* **2012**, *337*, 232−236.

(4) Jazayeri, A.; Andrews, S. P.; Marshall, F. H. Structurally enabled discovery of adenosine A_{2A} receptor antagonists. *Chem. Rev.* **2017**, *117*, 21−37.

(5) Fredholm, B. B.; IJzerman, A. P.; Jacobson, K. A.; Klotz, K.-N.; Linden, J. International Union of Pharmacology. XXV. Nomenclature and classification of adenosine receptors. *Pharmacol. Rev.* **2001**, *53*, 527−552.

(6) Rosentreter, U.; Henning, R.; Bauser, M.; Kraemer, T.; Vaupel, A.; Hübsch, W.; Dembowsky, K.; Salcher-Schräufstaetter, O.; Stasch, J.-P.; Krahn, T.; Perzborn, E. Substituted 2-thio-3,5-dicyano-4-aryl-6-aminopyridines and the use thereof as adenosine receptor ligands. World patent WO2001025210, April 12, 2001.

(7) Rosentreter, U.; Kraemer, T.; Shimada, M.; Huebsch, W.; Diedrichs, N.; Krahn, T.; K, H.; Stasch, J. Preparation of 2-heteroarylmethylthio-3,5-dicyano-4-phenyl-6-aminopyridines as adenosine receptor selective ligands. World patent WO03008384, January 30, 2003.

(8) Shah, S. J.; Voors, A. A.; McMurray, J. J. V.; Kitzman, D. W.; Viethen, T.; Bomfim Wirtz, A.; Huang, E.; Pap, A. F.; Solomon, S. D. Effect of neladenoson bialanate on exercise capacity among patients with heart failure with preserved ejection fraction: a randomized clinical trial. *JAMA* **2019**, *321*, 2101−2112.

(9) Betti, M.; Catarzi, D.; Varano, F.; Falsini, M.; Varani, K.; Vincenzi, F.; Dal Ben, D.; Lambertucci, C.; Colotta, V. The aminopyridine-3,5-dicarbonitrile core for the design of new non-nucleoside-like agonists of the human adenosine A_{2B} receptor. *Eur. J. Med. Chem.* **2018**, *150*, 127−139.

(10) Eckle, T.; Krahn, T.; Grenz, A.; Köhler, D.; Mittelbronn, M.; Ledent, C.; Jacobson, M. A.; Osswald, H.; Thompson, L. F.; Unertl, K.; Eltzschig, H. K. Cardioprotection by ecto-5′-nucleotidase (CD73) and A_{2B} adenosine receptors. *Circulation* **2007**, *115*, 1581−1590.

(11) Beukers, M. W.; Chang, L. C. W.; von Frijtag Drabbe Künzel, J. K.; Mulder-Krieger, T.; Spanjersberg, R. F.; Brussee, J.; IJzerman, A. P. New, non-adenosine, high-potency agonists for the human adenosine A_{2B} receptor with an improved selectivity profile compared to the reference agonist N-ethylcarboxamidoadenosine. *J. Med. Chem.* **2004**, *47*, 3707−3709.

(12) Guo, D.; Mulder-Krieger, T.; IJzerman, A. P.; Heitman, L. H. Functional efficacy of adenosine A_{2A} receptor agonists is positively correlated to their receptor residence time. *Br. J. Pharmacol.* **2012**, *166*, 1846−1859.
(13) Segala, E.; Guo, D.; Cheng, R. K. Y.; Bortolato, A.; Deflorian, F.; Doré, A. S.; Errey, J. C.; Heitman, L. H.; IJzerman, A. P.; Marshall, F. H.; Cooke, R. M. Controlling the dissociation of ligands from the adenosine A_{2A} receptor through modulation of salt bridge strength. *J. Med. Chem.* **2016**, *59*, 6470−6479.
(14) Rucktooa, P.; Cheng, R. K. Y.; Segala, E.; Geng, T.; Errey, J. C.; Brown, G. A.; Cooke, R. M.; Marshall, F. H.; Doré, A. S. Towards high throughput GPCR crystallography: In meso soaking of adenosine A_{2A} receptor crystals. *Sci. Rep.* **2018**, *8*, 41.
(15) Ballesteros, J. A.; Weinstein, H. [19] Integrated methods for the construction of three-dimensional models and computational probing of structure-function relations in G protein-coupled receptors. *Methods Neurosci* **1995**, *25*, 366−428.
(16) Lane, J. R.; Klein Herenbrink, C.; van Westen, G. J. P.; Spoorendonk, J. A.; Hoffmann, C.; IJzerman, A. P. A novel nonribose agonist, LUF5834, engages residues that are distinct from those of adenosine-like ligands to activate the adenosine A_{2A} receptor. *Mol. Pharmacol.* **2012**, *81*, 475−487.
(17) Gao, Z.-G.; Jiang, Q.; Jacobson, K. A.; IJzerman, A. P. Site-directed mutagenesis studies of human A_{2A} adenosine receptors: involvement of Glu^{13} and His^{278} in ligand binding and sodium modulation. *Biochem. Pharmacol.* **2000**, *60*, 661−668.
(18) Lebon, G.; Warne, T.; Edwards, P. C.; Bennett, K.; Langmead, C. J.; Leslie, A. G. W.; Tate, C. G. Agonist-bound adenosine A_{2A} receptor structures reveal common features of GPCR activation. *Nature* **2011**, *474*, 521−525.
(19) Bertheleme, N.; Singh, S.; Dowell, S. J.; Hubbard, J.; Byrne, B. Loss of constitutive activity is correlated with increased thermostability of the human adenosine A_{2A} receptor. *Br. J. Pharmacol.* **2013**, *169*, 988−998.
(20) Louvel, J.; Guo, D.; Agliardi, M.; Mocking, T. A. M.; Kars, R.; Pham, T. P.; Xia, L.; de Vries, H.; Brussee, J.; Heitman, L. H.; IJzerman, A. P. Agonists for the adenosine A_1 receptor with tunable residence time. A case for nonribose 4-amino-6-aryl-5-cyano-2-thiopyrimidines. *J. Med. Chem.* **2014**, *57*, 3213−3222.
(21) Chaplen, P.; Slack, R.; Wooldridge, K. R. H. 843. Isothiazoles. Part VII. Quaternary isothiazoles. *J. Chem. Soc.* **1965**, 4577−4578.
(22) Viira, B.; Selyutina, A.; García-Sosa, A. T.; Karonen, M.; Sinkkonen, J.; Merits, A.; Maran, U. Design, discovery, modelling, synthesis, and biological evaluation of novel and small, low toxicity s-triazine derivatives as HIV-1 non-nucleoside reverse transcriptase inhibitors. *Bioorg. Med. Chem.* **2016**, *24*, 2519−2529.
(23) Rudorf, W.-D.; Augustin, M. Acylketen-S,S- und Acylketen-S,N-acetale als Bausteine für Heterocyclen: 5-Cyanopyrimidine. *J. Prakt. Chem.* **1978**, *320*, 576−584.
(24) Suda, A.; Kawasaki, K.-I.; Komiyama, S.; Isshiki, Y.; Yoon, D.-O.; Kim, S.-J.; Na, Y.-J.; Hasegawa, K.; Fukami, T. A.; Sato, S.; Miura, T.; Ono, N.; Yamazaki, T.; Saitoh, R.; Shimma, N.; Shiratori, Y.; Tsukuda, T. Design and synthesis of 2-amino-6-(1H,3H-benzo[de]-isochromen-6-yl)-1,3,5-triazines as novel Hsp90 inhibitors. *Bioorg. Med. Chem.* **2014**, *22*, 892−905.
(25) Longstreet, A. R.; Campbell, B. S.; Gupton, B. F.; McQuade, D. T. Improved synthesis of mono- and disubstituted 2-halonicotinonitriles from alkylidene malononitriles. *Org. Lett.* **2013**, *15*, 5298−5301.
(26) Teague, S. J. Synthesis of heavily substituted 2-aminopyridines by displacement of a 6-methylsulfinyl group. *J. Org. Chem.* **2008**, *73*, 9765−9766.
(27) Doebelin, C.; Wagner, P.; Bertin, I.; Simonin, F.; Schmitt, M.; Bihel, F.; Bourguignon, J.-J. Trisubstitution of pyridine through sequential and regioselective palladium cross-coupling reactions affording analogs of known GPR54 antagonists. *RSC Adv.* **2013**, *3*, 10296−10300.
(28) Capaldi, C.; Armani, E.; Hurley, C.; Avitabile-Woo, B. G.; Lanaro, R.; Jennings, N. S. (4-(([1,2,4]Triazolo[4,3-A]pyridine-6-yl)oxy)-1,2,3,4-tetrahydronaphthalen-1-yl) ureido derivatives as anti-inflammatory P38 MAPK inhibitors for treating diseases of the respiratory tract. World Patent WO2018224423, December 13, 2018.
(29) Kim, Y. K.; Park, S. Y.; Joo, H. W.; Choi, E. S. Biaryl derivatives as GPR120 agonists. World Patent WO2014209034, December 31, 2014.
(30) Pevet, I.; Brulé, C.; Tizot, A.; Gohier, A.; Cruzalegui, F.; Boutin, J. A.; Goldstein, S. Synthesis and pharmacological evaluation of thieno[2,3-b]pyridine derivatives as novel c-Src inhibitors. *Bioorg. Med. Chem.* **2011**, *19*, 2517−2528.
(31) Roch, J.; Muller, E.; Narr, B.; Nickl, J.; Haarmann, W. 3-Amino-4-phenyl-6-piperidino-1H-pyrazolo[3,4-B]-pyridines and salts thereof. U.S. Patent US4,260,621, April 7, 1981.
(32) Hamidi, H.; Lilja, J.; Ivaska, J. Using xCELLigence RTCA instrument to measure cell adhesion. *Bio-Protoc.* **2017**, *7*, No. e2646.
(33) Chun, E.; Thompson, A. A.; Liu, W.; Roth, C. B.; Griffith, M. T.; Katritch, V.; Kunken, J.; Xu, F.; Cherezov, V.; Hanson, M. A.; Stevens, R. C. Fusion partner toolchest for the stabilization and crystallization of G protein-coupled receptors. *Structure* **2012**, *20*, 967−976.
(34) Sherman, W.; Day, T.; Jacobson, M. P.; Friesner, R. A.; Farid, R. Novel procedure for modeling ligand/receptor induced fit effects. *J. Med. Chem.* **2006**, *49*, 534−553.
(35) Xu, F.; Wu, H.; Katritch, V.; Han, G. W.; Jacobson, K. A.; Gao, Z.-G.; Cherezov, V.; Stevens, R. C. Structure of an agonist-bound human A_{2A} adenosine receptor. *Science* **2011**, *332*, 322−327.
(36) van Veldhoven, J. P. D.; Chang, L. C. W.; von Frijtag Drabbe Künzel, J. K.; Mulder-Krieger, T.; Struensee-Link, R.; Beukers, M. W.; Brussee, J.; IJzerman, A. P. I. A new generation of adenosine receptor antagonists: from di- to trisubstituted aminopyrimidines. *Bioorg. Med. Chem.* **2008**, *16*, 2741−2752.
(37) Kabsch, W. Integration, scaling, space-group assignment and post-refinement. *Acta Cryst.* **2010**, *66*, 133−144.
(38) Vonrhein, C.; Tickle, I. J.; Flensburg, C.; Keller, P.; Paciorek, W.; Sharff, A.; Bricogne, G. Advances in automated data analysis and processing within autoPROC, combined with improved characterisation, mitigation and visualisation of the anisotropy of diffraction limits using STARANISO. *Acta Cryst.* **2018**, *A74*, a360.
(39) McCoy, A. J.; Grosse-Kunstleve, R. W.; Adams, P. D.; Winn, M. D.; Storoni, L. C.; Read, R. J. Phaser crystallographic software. *J. Appl. Cryst.* **2007**, *40*, 658−674.
(40) Afonine, P. V.; Grosse-Kunstleve, R. W.; Echols, N.; Headd, J. J.; Moriarty, N. W.; Mustyakimov, M.; Terwilliger, T. C.; Urzhumtsev, A.; Zwart, P. H.; Adams, P. D. Towards automated crystallographic structure refinement with phenix.refine. *Acta Cryst.* **2012**, *68*, 352−367.
(41) Bricogne, G.; Blanc, E.; Brandl, M.; Flensburg, C.; Keller, P.; Paciorek, W.; Roversi, P.; Sharff, A.; Smart, O. S.; Vonrhein, C.; Womack, T. O. *BUSTER version 2.11.7*; Global Phasing Ltd.: Cambridge, United Kingdom 2017.
(42) Park, J. H.; Kim, Y. K.; Lui, J. H.; Yu, E. S.; Lee, H. I.; Jung, H. K. Organic optoelectronic device and display apparatus. U.S. Patent US2,017,331,067, November 16, 2017.
(43) Reimschuessel, H. K.; McDevitt, N. T. Infrared spectra of some 1,3,5-triazine derivatives. *J. Am. Chem. Soc.* **1960**, *82*, 3756−3762.
(44) Joshua, C. P.; Rajan, V. P. Interaction of dicyandiamides with thioamides: Formation of 6-Alkyl(or aryl)-4-amino(or arylamino)-1,3,5-triazine-2-thiols and amidino(or aryamidino)thioureas. *Aust. J. Chem.* **1972**, *27*, 2627−2634.
(45) Fryszman, O. M.; Lang, H.; Lan, J.; Chang, E.; Fang, Y. 5-Membered heterocycle-based P38 kinase inhibitors. World Patent WO2005009973, February 3, 2005.
(46) Borroni, E.; Hubert-Trottmann, G.; Kilpatrick, G.; Norcross, R. Adenosine receptor ligands and their use in the treatment of disease. U.S. Patent US20,010,027,196, October 4, 2001.
(47) Perez, M. A.; Soto, J. L.; Carrillo, J. R. A simple, unambiguous synthesis of 2-amino-4-oxo- and −4-thioxo-3,4-dihydropyrimidine-5-carbonitriles. *Synthesis* **1983**, *5*, 402−404.

https://doi.org/10.1021/acs.jmedchem.0c01856
J. Med. Chem. 2021, 64, 3827−3842

(48) Peseke, K.; Suarez, J.; Quincoces, J. Push-pull-butadiene; Synthese von 2-Amino-4-aryl(fur-2-yl)-6-methylthio-pyridin-3-carbonitrilen. *Zeitschrift fur Chemie* **1983**, *23*, 404−405.
(49) Mello, J. V.; Finney, N. S. Convenient synthesis and transformation of 2,6-dichloro-4-iodopyridine. *Org. Lett.* **2001**, *3*, 4263−4265.
(50) Smith, P. K.; Krohn, R. I.; Hermanson, G. T.; Mallia, A. K.; Gartner, F. H.; Provenzano, M. D.; Fujimoto, E. K.; Goeke, N. M.; Olson, B. J.; Klenk, D. C. Measurement of protein using bicinchoninic acid. *Anal. Biochem.* **1985**, *150*, 76−85.
(51) Xi, B.; Yu, N.; Wang, X.; Xu, X.; Abassi, Y. The application of cell-based label-free technology in drug discovery. *Biotechnol. J.* **2008**, *3*, 484−495.
(52) Yu, N.; Atienza, J. M.; Bernard, J.; Blanc, S.; Zhu, J.; Wang, X.; Xu, X.; Abassi, Y. A. Real-time monitoring of morphological changes in living cells by electronic cell sensor arrays: an approach to study G protein-coupled receptors. *Anal. Chem.* **2006**, *78*, 35−43.
(53) Schrödinger, LLC. *Small-Molecule Drug Discovery Suite 2018-4*; Schrödinger, LLC: New York, 2018.
(54) Jacobson, M. P.; Pincus, D. L.; Rapp, C. S.; Day, T. J. F.; Honig, B.; Shaw, D. E.; Friesner, R. A. A hierarchical approach to all-atom protein loop prediction. *Proteins* **2004**, *55*, 351−367.
(55) Schrödinger, LLC. *LigPrep Schrödinger Release 2019−1*; Schrödinger, LLC: New York, 2019.
(56) Schrödinger, LLC. *The PyMOL Molecular Graphics System, 2.2.2*; Schrödinger, LLC: New York, 2018.
(57) Cheng, Y.-C.; Prusoff, W. H. Relationship between the inhibition constant (K_I) and the concentration of inhibitor which causes 50 per cent inhibition (I_{50}) of an enzymatic reaction. *Biochem. Pharmacol.* **1973**, *22*, 3099−3108.
(58) Kourounakis, A.; Visser, C.; de Groote, M.; IJzerman, A. P. Differential effects of the allosteric enhancer (2-amino-4,5-dimethyl-trienyl)[3-trifluoromethyl phenyl]methanone (PD81,723) on agonist and antagonist binding and function at the human wild-type and a mutant (T277A) adenosine A_1 receptor. *Biochem. Pharmacol.* **2001**, *61*, 137−144.

https://doi.org/10.1021/acs.jmedchem.0c01856
J. Med. Chem. 2021, 64, 3827−3842